Journal of Medicinal Chemistry

ARTICLE

pubs.acs.org/jmc

Small Molecule Agonists of the Orphan Nuclear Receptors Steroidogenic Factor-1 (SF-1, NR5A1) and Liver Receptor Homologue-1 (LRH-1, NR5A2)

Richard J. Whitby,*[,†] Jozef Stec,[†] Raymond D. Blind,[‡] Sally Dixon,[†] Lisa M. Leesnitzer,[§] Lisa A. Orband-Miller,[§] Shawn P. Williams,[§] Timothy M. Willson,[§] Robert Xu,[§] William J. Zuercher,[§] Fang Cai,[‡] and Holly A. Ingraham[‡]

[†]School of Chemistry, University of Southampton, Southampton, Hants, SO17 1BJ, United Kingdom

[‡]Department of Cellular and Molecular Pharmacology, Mission Bay Campus, University of California San Francisco, San Francisco, California 94598, United States

[§]Molecular Discovery Research, GlaxoSmithKline, 5 Moore Drive, Research Triangle Park, North Carolina 27709-3398, United States

Supporting Information

ABSTRACT:

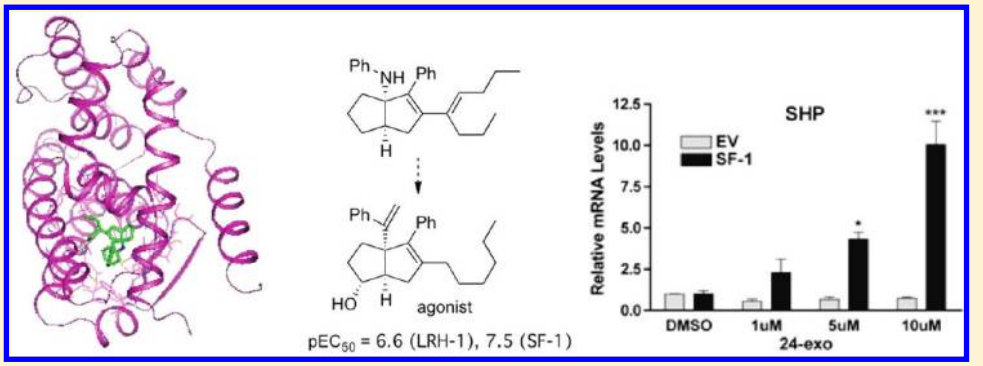

The crystal structure of LRH-1 ligand binding domain bound to our previously reported agonist 3-(*E*-oct-4-en-4-yl)-1-phenylamino-2-phenyl-*cis*-bicyclo[3.3.0]oct-2-ene **5** is described. Two new classes of agonists in which the bridgehead anilino group from our first series was replaced with an alkoxy or 1-ethenyl group were designed, synthesized, and tested for activity in a peptide recruitment assay. Both new classes gave very active compounds, particularly against SF-1. Structure−activity studies led to excellent dual-LRH-1/SF-1 agonists (e.g., RJW100) as well as compounds selective for LRH-1 (RJW101) and SF-1 (RJW102 and RJW103). The series based on 1-ethenyl substitution was acid stable, overcoming a significant drawback of our original bridgehead anilino-substituted series. Initial studies on the regulation of gene expression in human cell lines showed excellent, reproducible activity at endogenous target genes.

INTRODUCTION

The nuclear receptor (NR) superfamily in mammals comprises a highly conserved group of 49 receptors that act as transcription factors to regulate development, homeostatic physiology, and cellular metabolism.[1] Nearly half of all NRs are ligand regulated, responding to dietary or endocrine signals such as steroid hormones, retinoids, vitamin D, fatty acids, and thyroid hormone. As such, NRs are attractive targets for drug discovery,[2] and indeed, 13% of current FDA-approved drugs regulate NRs.[3] NRs without assigned natural ligands are referred to as orphan NRs.[4] On the basis of structural analyses of nearly all NR subfamilies, it is predicted that most orphan receptors might accommodate ligands, thus providing novel targets for pharmaceuticals. Finding natural or synthetic regulatory ligands for these orphan receptors is key to understanding their role in physiology,[5] a process termed "reverse endocrinology".[6] Attempts to "adopt" (or deorphanize) orphan NRs have been successful for NR1H4 (farnesoid X receptor, FXR)[7] and peroxisome proliferator-activated receptor family (PPARs, NR1Cs)[8] and have led to useful therapeutics.

Here, we have undertaken an effort to identify synthetic ligands for subfamily V members, including steroidogenic factor-1 (SF-1, NR5A1),[9] and its close homologue, liver receptor homologue-1 (LRH-1, NR5A2).[10] Both receptors are known to play important roles during embryonic development and in adult physiology.

Received: November 8, 2010
Published: March 10, 2011

dx.doi.org/10.1021/jm1014296 | *J. Med. Chem.* 2011, 54, 2266–2281

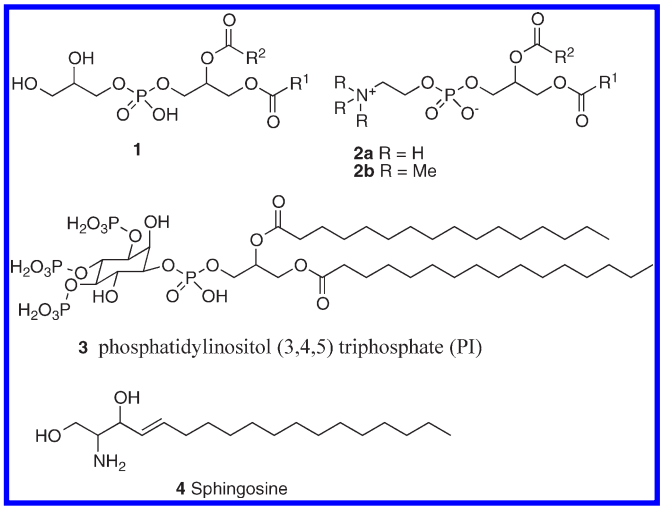

Figure 1. Natural ligands for LRH-1 or SF-1.

SF-1 (NR5A1) is a critical factor in vertebrate endocrine organ development, including male sexual differentiation, and is an important regulator of steroidogenic enzymes.[11] Numerous genetic mutations in the DNA binding domain (DBD) and ligand binding domain (LBD) of SF-1 correlate with abnormal testis development[12] and premature ovarian failure.[13] By contrast, amplification of SF-1 is associated with adrenocortical tumors, with inverse agonists reported to inhibit proliferation of primary cultured tumor cells.[14] SF-1 has also been implicated in the development of endometriosis and endometrial cancers.[15] Finally, rodent models suggest that SF-1 expressed in the hypothalamus influences anxiety, energy homeostasis, and appetite.[16]

LRH-1 plays a critical role in embryonic development of the endoderm[17] and is highly expressed in the intestine, liver, exocrine pancreas, and ovary.[18] LRH-1 regulates crucial enzymes in hepatic bile acid biosynthesis[19] and cholesterol homeostasis[10] and is a key controller in the hepatic acute phase response.[20] Thus, this receptor may be a target for the treatment of cardiovascular disease[21] and cholinostatic liver disease.[22] LRH-1 and SF-1 both regulate aromatase expression,[23] and LRH-1 is expressed in several human breast cancer cell lines, suggesting that antagonists in combination with traditional aromatase inhibitors might be effective in reducing local concentrations of estrogen in human breast carcinomas.[24] Finally, LRH-1 is expressed in human intestinal crypt cells where it controls cell proliferation and differentiation.[25] Its expression[26] and potential role in gastric cancer[27] suggest that LRH-1 can influence tumor formation by accelerating the cell cycle and promoting inflammation.[28]

Both SF-1 and LRH-1 have emerged as potential stem cell factors because both can regulate expression of Oct-4, which is one of the four factors found to induce pluripotency of mouse embryonic fibroblasts.[17,29] Moreover, these two NRs can completely replace Oct-4 to reprogram murine somatic cells to induce pluripotent cells[30a] and are also potent inducers in the transition from an epiblast stem cell to ground state pluripotency (iPS).[30b] As such, identifying effective agonists to either SF-1 or LRH-1 might help in achieving a pharmaceutical approach in generating or maintaining pluripotent human stem cells.

LRH-1 and SF-1 bind to DNA as monomers and show constitutive activity when expressed in a variety of cell types.[9,10] Receptor activity can be regulated by post-translational modifications including phosphorylation[31] and sumoylation[32] or through

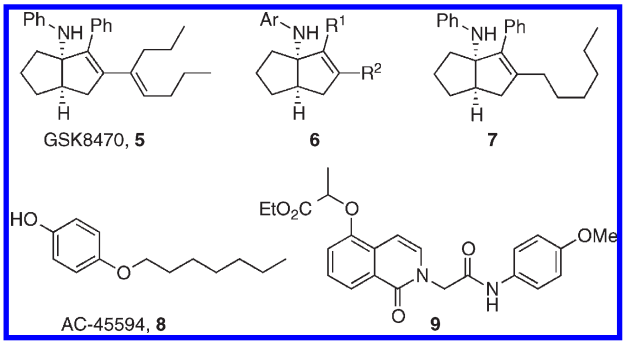

Figure 2. Synthetic compounds reported to modulate SF-1 or LRH-1 activity.

interaction with the atypical orphan receptors that lack a DBD, including small/short heterodimer partner (SHP, NR0B1)[33] and DAX-1, Dosage-sensitive sex reversal, adrenal hypoplasia critical region, on chromosome X, gene 1) (NR0B2).[34]

X-ray crystallography coupled with mass spectroscopy revealed the presence of *Escherichia coli*-derived phospholipids, phosphatidylglycerides (**1**; Figure 1) and phosphatidylethanolamines (**2a**) in the ligand binding pockets of human LRH-1 and SF-1.[35] The majority of phospholipids bound to either SF-1 or human LRH-1 LBD were identified as having C16 or 18 acyl groups with some showing a *cis*-alkene in the Δ9 position. Whether these phospholipids merely serve as structural ligands or serve a regulatory role remains to be established. Support for phospholipids as regulatory ligands includes increased coactivator peptide recruitment on binding of phospholipids to SF-1[35c] and a correlation between binding of phospholipid and LRH-1-induced activation of gene expression.[35d] The exchange of bacterially derived phosphatidyl glyceride (**1**) with phospholipids such as **3**[35b] and phosphatidycholine (**2b**) has been demonstrated.[36] In the latter case, the exchange had little effect on binding of coactivator peptides.[36] Recently, Moore has claimed in a patent that diundecanoyl (**2b**, $R^1 = R^2 = nC_9H_{19}$) and dilauroyl (**2b**, $R^1 = R^2 = nC_{11}H_{23}$) phosphatidylcholine (PC) act as agonists of the LRH-1 receptor and that administration of these lipids to diabetic mice reduces blood glucose levels.[37] Other correlative data include the finding that SF-1 activation by a tamoxifen analogue increases cellular levels of phosphatidylinositol (3,4,5) triphosphate (**3**).[15c] Finally sphingosine (**4**) is reported to bind SF-1 and suppress expression of the SF-1 target gene CYP17a1.[38] Derivatives of (**4**) such as sphingosylphosphorylcholine and *N*-Acyl-**4** (ceramides) may also be natural ligands.

We reported the first synthetic small molecule agonist for LRH-1 and SF-1, GSK8470 (**5**), and a structure−activity relationship (SAR) study on the series **6** leading to the more active analogue **7** (Figure 2).[39] Another small molecule known to activate both SF-1 and LRH-1 is the herbicide atrazine,[40] but the precise mechanism leading to this increased receptor activity has yet to be defined.

Recently, *p*-heptyloxyphenol (**8**) was reported as a potent (IC_{50} = 7.3 μM) inverse agonist for SF-1 but with no activity against LRH-1.[41] Expression of several reported SF-1 target genes was suppressed by **8** in cell-based assays. However, although **8** was reported to inhibit proliferation of adrenocortial carcinoma cell line H295R, it had the same effect with an SF-1 negative cell line (SW-13).[14] Several isoquinoline-based inverse agonists of SF-1 were discovered through high-throughput screening and

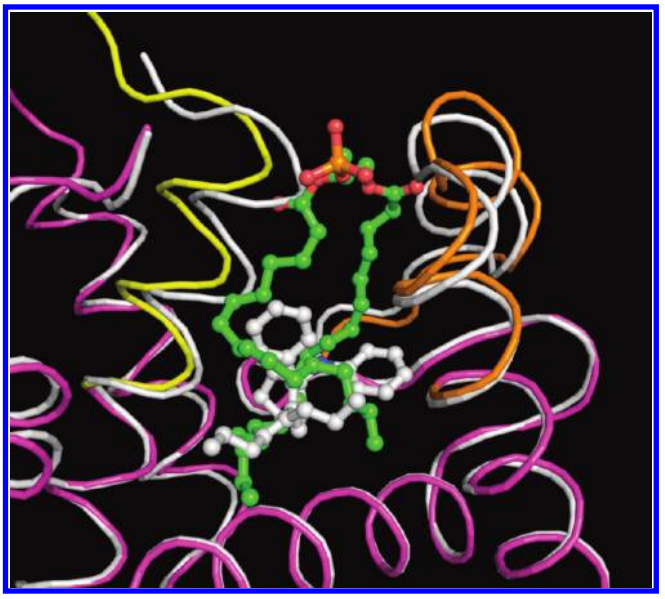

Figure 3. Cα trace from the phospholipid[35b] (magenta, orange, and yellow) and **5** (white) bound conformations of LRH-1 were superimposed for comparison. The pocket contracts around the smaller **5**, with the biggest shifts occurring for residues 338−350 in helix 3 (yellow) and residues 408−427 in the β-turn and helix 6 (orange), where the phospholipid headgroup protrudes.

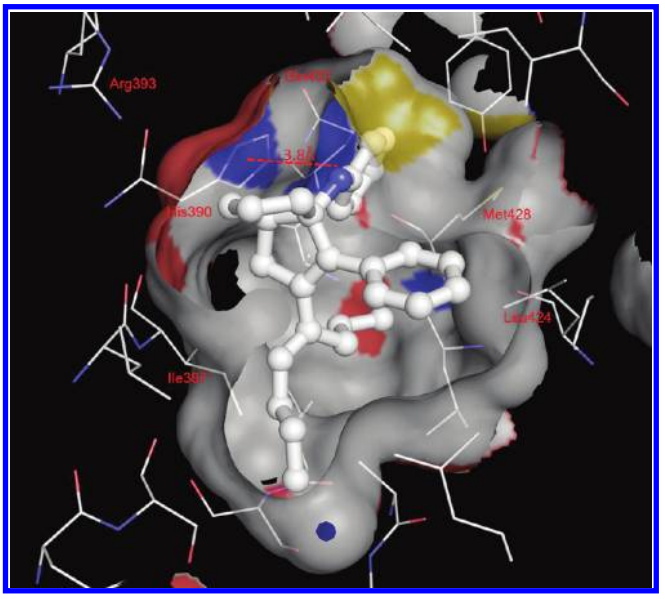

Figure 4. Compound **5** is shown in the LRH-1 ligand binding pocket. Contacting residues are indicated, along with the His390−aniline distance. The surface of the pocket is shown, colored by the nearest atom type. The region of the pocket adjacent to helix 5 and the β-turn contain polar residues and several trapped water molecules.

further SAR studies, of which **9** was most active (IC_{50} = 200 nM).[41,42] At high levels (10 μM), **9** modestly suppressed doxycycline (DOX) induced proliferation of H295R cell line with little effect on the SF-1 negative SW-13 cell line. Closely related isoquinolines affected both cell lines in a similar way, suggesting a non-SF-1 mechanism. The SAR for these series seems complex; for example, replacing the methoxy group in **9** with ethoxy gave a compound highly active against a range of

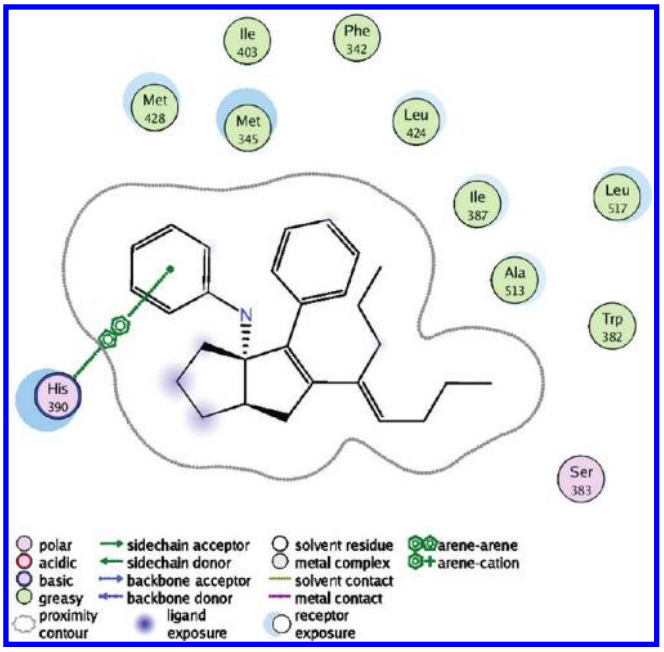

Figure 5. Two-dimensional compound interaction diagram depicting adjacent residues and the π stacking interaction with His390. The crystal structure is available from the RCSB with access code 3PLZ and is further described in the Experimental Section.

other receptors and exhibiting strong cell toxicity, suggesting transactivation assay artifacts (promiscuous inhibition of the reporter system).

Although **5** and related compounds **6** have proven to be excellent biological probes for LRH-1 and SF-1, they have a number of limitations. Most important is that they are unstable to acid, making handling difficult and raising doubts about stability during biological application. The series also shows little discrimination between LRH-1 and SF-1. The aim of this work was thus first to develop new series of compounds that were more stable and easily handled than series **6**, but with at least comparable binding and efficacy, and second to find compounds that were selective for LRH-1 and/or SF-1.

■ COCRYSTAL STRUCTURE OF 5 WITH hLRH-1

As a basis for the design of improved analogues of **5**, we solved the cocrystal structure of compound **5** bound to the human LRH-1 LBD (Figures 3 and 4). Although racemic **5** was used, the 1*S*,5*R*-bicyclo[3.3.0]oct-2-ene enantiomer cocrystallized with LRH-1 LDB. Compound **5** occupied the same binding pocket volume as the terminal 12 carbon atoms in both acyl chains of a phospholipid bound in LRH-1.[35b] This smaller size permitted LRH-1 to contract, narrowing the gap between the N-terminal half of helix 3 (residues 338−350, yellow in the PL-bound structure) and the β-turn/helix 6 region (residues 408−427, orange in the PL-bound structure) where the phospholipid headgroup is situated in the PL + LRH-1 structure, and completely enclose the ligand within the binding pocket. Making no polar interactions with the protein, **5** was a compact, hydrophobic mass complementing the inner surface of the binding pocket. There was π stacking between the His390 and the aniline of **5** with a centroid−centroid distance of 3.8 Å and a deviation from coplanarity of around 10°.

dx.doi.org/10.1021/jm1014296 |*J. Med. Chem.* 2011, 54, 2266–2281

The structure suggested some chemical strategies for improving compound properties. The acid-labile aniline nitrogen made no polar interactions with the protein, suggesting that another more stable linker might be tolerated. We thus designed compounds with oxygen- and carbon-based linkages from the substituted bridgehead carbon. Additionally, His390, Arg393, and Gln432 were within 5 Å of the compound. Polar moieties could be incorporated to interact with these residues, which might both improve binding and increase hydrophilicity of the ligand (Figure 5).

CHEMISTRY

Alkoxy-Substituted Series. Racemic tertiary alcohol **11** was synthesized as previously reported[39] from hept-6-en-1-yn-1-ylbenzene via Pauson−Khand cyclization to give the cyclopentenone **10** and cerium trichloride-assisted 1,2-addition of hexylmagnesium bromide (Scheme 1). Exposure of **11** to various alcohols in the presence of catalytic amounts of camphorsulphonic acid gave a series of racemic analogues **12** of **7** in which an alkoxy group replaced the aniline substituent. Yields for the last step were generally good (Table 1), the exception being when the alcohol carried an α-branch. The products **12** were unstable to silica, so were purified by column chromatography on basic grade III alumina.

"All Carbon" Series. A previously reported[43] tandem reaction sequence on zirconocene was used to construct "all carbon" analogues **18** of **7**. Thus, intramolecular cocyclization of 1,6-enyne

Scheme 1. Preparation of Bridgehead-Alkoxy Series[a]

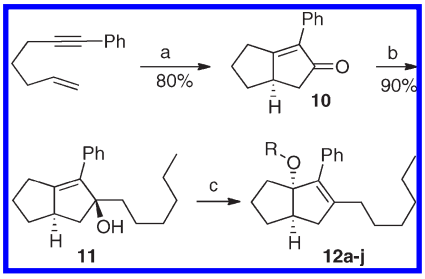

[a] Reagents and conditions: (a) $Co_2(CO)_8$, DMSO (10 equiv), THF, reflux, 5 h, 80%. (b) $nC_6H_{13}MgBr$, $CeCl_3$, −10 °C to room temperature, 1 h, 90%. (c) ROH (10 equiv), camphorsulfonic acid (0.1 equiv), 20 °C, 3.5 h.

Table 1. Synthesis of 1-Alkoxy-3-hexyl-2-phenyl-*cis*-bicyclo[3.3.0]oct-2-enes 12a−j

compound	R	yield (%)[a]
12a	Me	75
12b	Et	69
12c	*n*Pr	71
12d	*i*Pr	7
12e	*n*Bu	68
12f	$CH_2CH(Me)(Et)$	64
12g	*n*Pent	62
12h	*n*Hex	65
12i	*c*Hex	12
12j	CH_2Ph	69

[a] Isolated yield from **11**.

Scheme 2. Preparation of Bridgehead 1-Alken-2-yl-Substituted Systems[a]

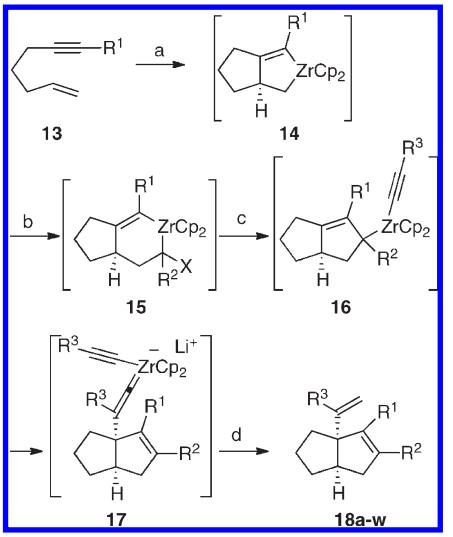

[a] Reagents and conditions: (a) (i) Cp_2ZrBu_2, THF, −78 °C, 0.5 h; (ii) room temperature, 2 h. (b) R^2CHX_2 (X = Br for R^2 = *n*Hex, *n*Bu, *n*Oct; X = Cl for R^2 = H, $SiMe_2Ph$), LDA or LiTMP, −78 °C, 15 min. (c) $R^3C{\equiv}CLi$ (3 equiv), −78 to −60 °C over 0.5 h. (d) MeOH, $NaHCO_3$, room temperature, 12−16 h.

Table 2. Synthesis of 1-(2-Alkenyl)-bicyclo[3.3.0]oct-2-enes 18

	R^1	R^2	R^3	yield (%)[a]
18a	Ph	*n*Hex	Ph	86
18b	Ph	*n*Hex	3-MeOPh	78
18c	Ph	*n*Hex	4-MeOPh	72
18d	Ph	*n*Hex	4-MePh	62
18e	Ph	*n*Hex	4-EtPh	70
18f	Ph	*n*Hex	4-*n*BuPh	78
18g	Ph	*n*Hex	4-*t*BuPh	51
18h	Ph	*n*Hex	4-PhPh	60
18i	Ph	*n*Hex	*n*Pr	54
18j	Ph	*n*Hex	*n*Bu	75
18k	Ph	*n*Hex	*n*Hex	65
18l	Ph	*n*Hex	*n*Oct	56
18m	3-MeOPh	*n*Hex	Ph	75
18n	4-EtPh	*n*Hex	Ph	70
18o	*n*Pr	*n*Hex	Ph	82
18p	*n*Bu	*n*Hex	Ph	88
18q	*n*Hex	*n*Hex	Ph	86
18r	*c*Hex	*n*Hex	Ph	80
18s	$(CH_2)_3OH$	*n*Hex	Ph	61
18t	Ph	H	Ph	58
18u	Ph	*n*Bu	Ph	71
18v	Ph	*n*Oct	Ph	73
18w	Ph	$SiMe_2Ph$	Ph	45

[a] Isolated yield of >95% pure material.

13 gave the zirconacyclopentenes **14** (Scheme 2). The addition of a 1,1-dihaloalkyl compound followed by lithium diisopropylamide (LDA) or lithium 2,2,6,6-tetramethylpiperidide (LiTMP) generated a carbenoid R^2X_2CLi in situ, which when inserted into

dx.doi.org/10.1021/jm1014296 |J. Med. Chem. 2011, 54, 2266–2281

Scheme 3. Preparation of Cyclohexyl- and Pyrrolidine-Fused Systems[a]

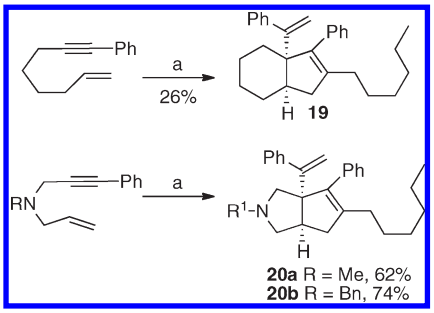

[a] Reagents and conditions: (a) (i) Cp_2ZrBu_2, THF, −78 °C, 0.5 h; (ii) room temperature, 2 h; (iii) *n*HexCHBr$_2$, LDA, −78 °C, 15 min; (iv) PhC≡CLi (3 equiv), −78 to −60 °C over 0.5 h; (v) MeOH, $NaHCO_3$, room temperature, 12−16 h.

Scheme 4. Preparation of 6-Oxygenated Systems[a]

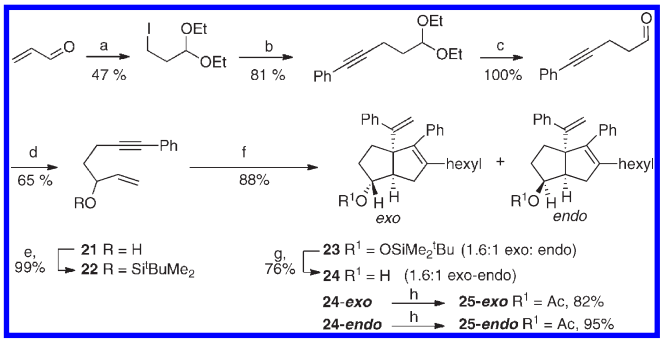

[a] Reagents and conditions: (a) (i) NaI, Me_3SiCl, MeCN; (ii) EtOH, 0 °C to room temperature, 2 h. (b) PhC≡CLi (1.5 equiv), THF, HMPA (1.5 equiv), −78 °C, 1 h then room temperature, 14 h. (c) THF:H_2O (4:1), HCl (2 M), room temperature, 3 h. (d) (i) $CH_2CHMgBr$, −78 to −65 °C, 1 h; (ii) NH_4Cl(aq). (e) *t*BuMe_2SiOTf, imidazole, DMAP, THF, room temperature, 18 h. (f) (i) Cp_2ZrBu_2, THF −78 °C, 0.5 h then 3 h at room temperature; (ii) −78 °C, *n*HexCHBr$_2$, LDA, 15 min; (iii) PhC≡CLi (3.0 equiv), −78 °C to −60 °C over 45 min; (iv) MeOH/$NaHCO_3$(aq), room temperature, 5 h. (g) TBAF (5 equiv), THF, room temperature, 20 h. (h) Pyridine, Ac_2O (73 equiv), DMAP (0.58 equiv), 13 h.

the alkyl-zirconium bond of **14** afforded the ring-expanded zirconacyclohexene **15**. The addition of a lithiated alkyne induced a ring-closing rearrangement to the bicyclo[3.3.0]oct-1-ene **16**, which rearranged further to the zirconocene alkylideneate complex **17**, incorporating a second alkyne moiety. Aqueous workup gave the racemic 1-(2-alkenyl)-bicyclo[3.3.0]oct-2-enes **18a**−**w** in generally excellent yield (Table 2) for a single-pot, three-component coupling. The yields were poorer when dichloromethane was the carbenoid precursor due to bis- and tris-insertion of the derived carbenoid into the zirconacycle.

The tandem reaction sequence also worked for the formation of the racemic bicyclo[4.3.0]non-8-ene **19** and pyrrolidine fused systems **20a**,**b** (Scheme 3). The low yield for compound **19** reflected a difficult separation from by-products —the yield estimated from the partially purified product was 46%.[44]

Compounds carrying oxygen substitution on the saturated cyclopentane ring were required. The synthesis of the 6-oxygenated compounds is shown in Scheme 4.

Scheme 5. Preparation of 7-Oxygenated Systems[a]

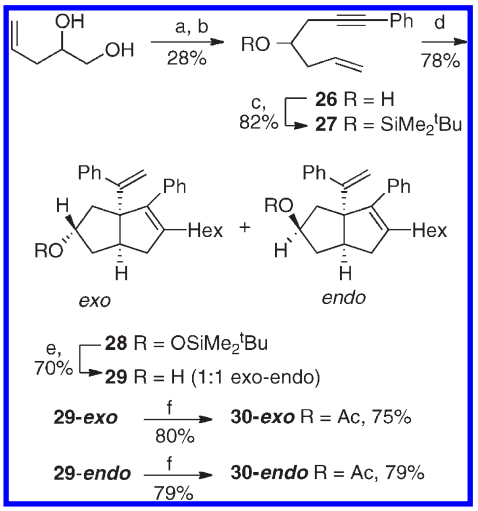

[a] Reagents and conditions: (a) (i) NaH, THF, −10 °C; (ii) *N*-tosyl imidazole, −10 °C, 1 h. (b) PhC≡CLi (2 equiv), THF, HMPA (2 equiv), −10 to 0 °C over 1 h then room temperature, 40 h; (iii) saturated $NaHCO_3$(aq). (c) Me_2*t*BuSiOTf, imidazole, DMAP, THF, room temperature, 15 h. (d) (i) Cp_2ZrBu_2, −78 °C, 0.5 h then 3 h at room temperature; (ii) *n*HexCHBr$_2$, LDA, −78 °C; (iii) PhC≡CLi (3 equiv), −78 °C to −60 °C over 45 min; (iv) MeOH/$NaHCO_3$(aq), room temperature, 5 h. (e) TBAF (2 equiv), THF, room temperature, 20 h. (f) Pyridine, Ac_2O (75 equiv), DMAP (0.58 equiv), room temperature, 17 h.

Using ethanol and in situ-generated Me_3SiI, acrolein was converted into 1,1-diethoxy-3-iodopropane,[45] which after rapid purification by chromatography on basic alumina (grade III) was reacted with lithium phenylacetylide to give (5,5-diethoxypent-1-yn-1-yl)benzene. Hydrolysis of the acetal to give an aldehyde was followed by reaction with vinylmagnesium bromide to afford the alcohol **21**. Protection of the hydroxyl group with *t*BuMe_2SiOTf gave the desired cyclization precursor **22**, which underwent the zirconocene-induced cocyclization, carbenoid insertion, and phenyl acetylide addition to give a 1.6:1 mixture of the *exo* and *endo* isomers **23** after protonolysis. Tetrabutylammonium fluoride (TBAF) cleavage of the silyl group furnished the desired racemic bicyclic alcohols **24**. The *exo* and *endo* isomers were separated by careful chromatography on silica, with the *endo* isomer eluting first. The relative stereochemistries of the *exo* and *endo* isomers were clear from coupling patterns to the proton adjacent to the hydroxyl group. In the *endo* isomer, it appears as a ddd, J = 9.1, 8.5, 5.5 Hz, and in the *exo* isomer, it appears as a broad singlet, the patterns being in accord with expectations from molecular modeling and the Karplus relationship of couplings to dihedral angles.[46] The separated diastereoisomers of **24** were acylated to afford **25**-*endo* and **25**-*exo*. A crystal structure of **25**-*endo* confirmed the stereochemical assignment.[47] The 7-oxygenated series was synthesized as shown in Scheme 5.

A single-pot ring-closure/ring-opening procedure was used to convert pent-4-ene-1,2-diol[48] into alcohol **26**.[49] Thus, selective tosylation of the primary alcohol was followed by in situ ring closure to an epoxide and ring-opening with lithium phenylacetylide to afford the alcohol **26**.[50] The overall yield was poor despite considerable optimization. *t*BuMe_2Si (TBDMS) protection of **26** gave **27**, which underwent zirconocene-mediated cocyclization, dibromocarbenoid insertion, and phenylacetylide-driven

dx.doi.org/10.1021/jm1014296 |*J. Med. Chem.* 2011, 54, 2266–2281

Table 3. Correlation between Predicted and Observed Coupling Constants for 29

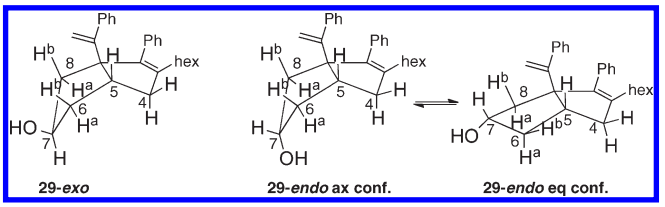

between	H^7-H^{8b}	H^7-H^{8a}	H^7-H^{6b}	H^7-H^{6a}	$H^{6b}-H^5$	$H^{6a}-H^5$
			29-*exo*			
dihedral angle (°)	164	47	154	37	14	104
calcd ^3J (Hz)	10.2	6.1	8.9	7.6	9.7	1.9
observed ^3J (Hz)	8.5	5.5	8.3	6.3	10	3.6
			29-*endo* ax. conf.			
dihedral angle (°)	38	80	33	87	18	101
calcd ^3J (Hz)	5	1.3	5.9	1.3	9.4	1.6
			29-*endo* eq. conf.			
dihedral angle (°)	44	159	46	165	35	155
calcd ^3J (Hz)	6.6	9.5	6.3	10.4	7.3	10.5
average calcd **29**-*endo* eq. and −ax. conf. ^3J (Hz)	5.8	5.4	6.1	5.9	8.4	6.1
observed ^3J (Hz)	6.2	4.6	5.6	5	9.5	6

zirconate rearrangement to give a 1:1 mixture of the *exo* and *endo* isomers **28**. After TBAF cleavage of the silyl group, the racemic *exo* and *endo* isomers of **29** were separated by careful chromatography, with the *endo* isomer eluting first. Acylation of the separated diastereoisomers furnished **30**-*exo* and **30**-*endo*.

The relative stereochemistries of **29**-*exo* and **29**-*endo* (and hence **30**-*exo* and **30**-*endo*) were established by nuclear magnetic resonance (NMR) studies combined with molecular modeling (Table 3) using the MMFF94 force field as implemented in Spartan 06 (Wavefunction Inc.).[51] The proton next to the hydroxyl group in one isomer appeared as a tt, J = 8.5, 5.9 Hz (due to couplings of 8.5, 8.3, 6.3, and 5.5 Hz), consistent with **29**-*exo* or the equatorial conformer of **29**-*endo* (**29**-*endo* eq. conf.), but as a quintet (J = 5.5 Hz) in the other diastereoisomer, not consistent with any minimum energy structure. Molecular modeling showed that **29**-*exo* had a well-defined minimum energy conformer, but for **29**-*endo*, the "equatorial" and "axial" hydroxy conformers (**29**-*endo* eq. and **29**-*endo* ax.) were <1 kJ/mol different in energy. The expected coupling patterns for each conformer of **29**-*endo* were calculated using the Altona modification[46b] of the Karplus relationship[46a] between dihedral angle and ^3J as implemented in the Mspin program[52] from Mestrec. The average showed a good correlation to the observed coupling constants (Table 3).

Stability Tests. Compounds **18a**, **24**-*exo*, **24**-*endo*, **28**-*exo*, and **28**-*endo* were stable after being kept in $CDCl_3$ at room temperature in the presence of daylight for 2 weeks or being exposed to 1.0 equiv of (+)-camphorsulfonic acid in $CDCl_3$ at room temperature for 1 week.

RESULTS AND DISCUSSION

The compounds **12a**−**j**, **18a**−**w**, **19**, **20a**,**b**, **24**, **25**, **29**, and **30** were screened for activity against both hLRH-1 and hSF-1 using fluorescence resonance energy transfer (FRET)-based peptide recruitment assay. Purified bacterial-expressed LBDs[35b] of human LRH-1 or human SF-1 were labeled with biotin and incubated with APC-labeled streptavidin (Molecular Probes). Peptides derived from TIF-2 amino acids 737−757 (B-QEPVSPKK-KENALLRYLLDKDDTKD-CONH2) for LRH-1 or from DAX-1 amino acids 1−23 (B-MAGENHQWQGSILYNMLMSAKQT-CONH2) for SF-1 were labeled with biotin and incubated with europium-labeled streptavidin (Perkin-Elmer, Wallac). The labeled receptor and peptide were incubated in the presence of various concentrations of test compound, and the associated complexes were quantified by time-resolved fluorescence energy transfer (TR-FRET). The pEC_{50} values of the test compounds, which serve as a measure of the binding affinity for the receptor, were estimated from a plot using the ratio of fluorescence values collected at 671 nm to fluorescence values collected 618 nm versus concentration of test compound added. Typically, 11 points over the concentration range 1 nm to 10 μM was used to construct each dose−response curve, and the pEC_{50} was calculated using ActivityBase 5.4 software. Six and three repeats were carried out for LRH-1 and SF-1, respectively. Test compounds that increased the affinity of the receptors for the peptide yielded an increase in fluorescent signal. The dose−response curves were sigmoidal with a clear plateau at high concentrations of test compound, the level of which we report as the relative efficacy (RE) of peptide recruitment. In the absence of a known standard, the value of RE was normalized to **24**-*exo* for both LRH-1 and SF-1. The average standard deviations of the pEC_{50} values for LRH-1 and SF-1 were 0.07 and 0.08, respectively, hence, the retention of the first decimal place. The average standard deviations of the RE values for LRH-1 and SF-1 were 0.034 and 0.025, respectively, hence, the retention of the second decimal place in the reported values but with an approximately ±0.03 95% confidence limit.

dx.doi.org/10.1021/jm1014296 |J. Med. Chem. 2011, 54, 2266–2281

Table 4. LRH-1 and SF-1 Binding and Activation of Alkoxy-Substituted Series 12

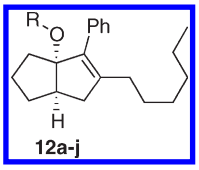

compound	R	pEC$_{50}$ (RE) LRH-1	pEC$_{50}$ (RE) SF-1
5		6.2 (0.89)	6.8 (0.36)
7		7.5 (0.38)	7.4 (0.70)
12a	Me	ia	ia
12b	Et	5.6 (0.17)	6.3 (0.55)
12c	*n*Pr	5.6 (0.21)	6.7 (0.67)
12d	*i*Pr	5.5 (0.19)	6.4 (0.49)
12e	*n*Bu	5.3 (0.39)	6.6 (0.62)
12f	$CH_2CH(Me)(Et)$	5.6 (0.18)	6.7 (0.56)
12g	*n*Pent	ia	6.4 (0.43)
12h	*n*Hex	ia	ia
12i	*c*Hex	6.1 (0.16)	7.1 (0.66)
12j	CH_2Ph	7.0 (0.13)	ia

Table 5. Variation of Bridgehead Substituent in Series 18 Compounds

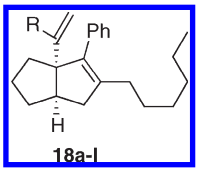

compound	R	pEC$_{50}$ (RE) LRH-1	pEC$_{50}$ (RE) SF-1
18a	Ph	6.6 (0.24)	7.2 (0.78)
18b	3-MeOPh	6.5 (0.25)	7.2 (0.28)
18c	4-MeOPh	ia	ia
18d	4-MePh	5.7 (0.25)	6.8 (0.28)
18e	4-EtPh	ia	ia
18f	4-*n*BuPh	6.0 (0.14)	ia
18g	4-*t*BuPh	ia	ia
18h	4-PhPh	ia	ia
18i	*n*Pr	5.5 (0.23)	6.8 (0.66)
18j (RJW102)	*n*Bu	5.6 (0.19)	6.7 (0.76)
18k	*n*Hex	ia	ia
18l	*n*Oct	ia	ia

The screening data are presented in several tables. Table 4 shows the alkoxy-substituted series **12a**−**j**, and Tables 5−7 show the series **18** compounds with emphasis on variation at the 1-, 2-, and 3-positions of the bicyclo[3.3.0]oct-2-ene skeleton, respectively. Table 8 contains the alternative core structures of **19** and **20**. Finally, Table 9 provides results from compounds **24**, **25**, **29**, and **30** with oxygen substitution on the cyclopentane ring.

Table 6. Variation of 2-Substituent in Series 18 Compounds

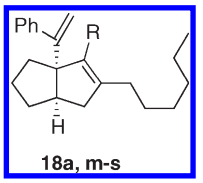

compound	R	pEC$_{50}$ (RE) LRH-1	pEC$_{50}$ (RE) SF-1
18a	Ph	6.6 (0.24)	7.2 (0.78)
18m	3-MeOPh	6.6 (0.13)	6.9 (0.42)
18n	4-EtPh	ia	ia
18o	*n*Pr	ia	6.4 (0.56)
18p	*n*Bu	ia	6.6 (0.59)
18q	*n*Hex	ia	ia
18r	*c*Hex	5.9 (0.15)	6.7 (0.59)
18s (RJW101)	$(CH_2)_3OH$	6.1 (0.38)	ia

Table 7. Variation of 3-Substituent in Series 18 Compounds

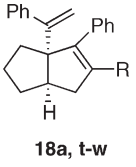

compound	R	pEC$_{50}$ (RE) LRH-1	pEC$_{50}$ (RE) SF-1
18a	*n*Hex	6.6 (0.24)	7.2 (0.78)
18t	H	ia	ia
18u	*n*Bu	6.7 (0.54)	7.4 (0.86)
18v	*n*Oct	5.8 (0.15)	6.8 (0.67)
18w	$SiMe_2Ph$	6.8 (0.53)	7.2 (0.33)

We were pleased to find that many of the alkoxy-substituted analogues were active against both LRH-1 and SF-1, showing that the nitrogen in the aniline series **6** (exemplified by **5** and **7**) was not necessary. All of the compounds (except **12j**) bound less strongly to LRH-1 and induced less recruitment of peptide than the aniline series, suggesting that an aromatic group is preferred by LRH-1 in this region. Unfortunately, it was not possible to make the OPh-substituted system as it was highly unstable, both because phenoxide is a much better leaving group than alkoxides but also because phenol will act as an acid catalyst for decomposition. The compounds showed good selectivity for SF-1, with binding approaching and efficacy exceeding that of our currently most used biological tool **5**. For both LRH-1 and SF-1, there is a clear SAR relating to the size of the R group with both small groups (Me) and large groups giving inactive compounds. The cutoff for large chains is sharp, indicating a defined pocket being

dx.doi.org/10.1021/jm1014296 |*J. Med. Chem.* 2011, 54, 2266–2281

Table 8. Effect of Variations in Skeleton on Biological Activity

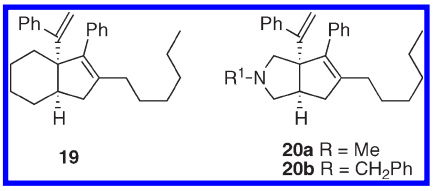

	pEC$_{50}$ (RE)	
compound	LRH-1	SF-1
18a	6.6 (0.24)	7.2 (0.78)
19	6.6 (0.23)	7.2 (0.42)
20a (RJW103)	5.9 (0.20)	6.5 (0.49)
20b	6.5 (0.13)	ia

Table 9. Effect of Oxygen Substitution on the Cyclopentane Ring

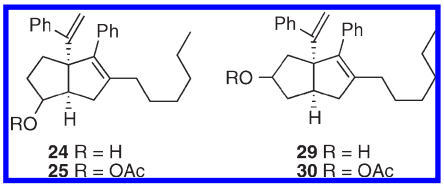

	pEC$_{50}$ (RE)	
compound	LRH-1	SF-1
18a	6.6 (0.24)	7.2 (0.78)
24-*exo* (RJW100)	6.6 (1.00)	7.5 (1.00)
24-*endo*	6.4 (0.67)	7.2 (0.77)
25-*exo*	6.4 (0.18)	6.4 (0.25)
25-*endo*	6.6 (0.18)	7.1 (0.24)
29-*exo*	6.0 (0.53)	6.6 (0.49)
29-*endo*	5.8 (0.33)	6.5 (0.95)
30-*exo*	ia	ia
30-*endo*	6.3 (0.13)	6.7 (0.34)

filled. For LRH-1, this is above four carbons long [cyclohexyl, $CH_2CH(Me)(Et)$, and *n*-butyl all fit, while *n*-pentyl does not]. For SF-1, the pocket appears slightly larger with *n*-pentyl, but not *n*-hexyl fitting. These results are comparable to those observed with aniline series **6**, compounds where 3- or 4-substitution on the NAr ring gave reduced binding or inactive compounds.[39] An interesting exception was the benzyloxy derivative **12j**, which displayed excellent binding to LRH-1, although poor efficacy, but was inactive against SF-1. It seems likely that π stacking with His-390 as described above for compound **5** results in the strong binding. Although the alkoxy-substituted series provided candidates for some of our key aims including the SF-1 and LRH-1 selective compounds **12g** and **12j**, respectively, these compounds proved as acid sensitive as the aniline series, as evidenced by their decomposition on attempted chromatography on silica or when stored in glassware that had not been washed with base.

The acid instability of series **12** prompted us to test compound **18a** with a similar *cis*-bicyclo[3.3.0]oct-2-ene structure but which lacked the acid-sensitive bridgehead leaving group, and it was found to exhibit good binding and activation of both LRH-1 and SF-1 (Table 5).

Variation of the lithiated alkyne used in the multicomponent synthesis of **18** allowed variation of the bridgehead substituent (Table 5). As with the series **12** compounds, we observe a strict cutoff in the size of group R, which can be accommodated. Even addition of a *para*-methyl group to the preferred phenyl substituent decreased binding (**18d**), and anything larger (**18e**−**h**) gave inactive compounds. The potent binding, although poor efficacy, of **18f** with LRH-1 is an anomaly and perhaps indicates an approach to developing reverse agonists of LRH-1. Interestingly, a 3-MeO group was well tolerated perhaps indicating some stabilization via dipolar interactions or weak H-bonding, whereas a 4-OMe substitution gave an inactive compound (**18c**). When R is an alkyl group (**18i**−**l**), LRH-1 binds only the shortest tried (R = *n*Pr, *n*Bu **18i**,**j**) and then with low pEC$_{50}$ and efficacy. The comparison of **18j** (R = *n*Bu) with the similarly sized but much more active **18a** (R = Ph) indicates a strong preference for an aryl group correlating with aromatic stacking with His390 noted in the crystal structure of LRH-1 and **5** above. SF-1 bound the R = *n*Bu compound **18j** strongly and with good efficacy, confirming the larger pocket noted in the SAR of series **12** and providing a good SF-1 selective analogue in the FRET assay. The longer chain compounds **18k** (R = *n*-hexyl) and **18i** (R = *n*-octyl) were inactive.

Changing the 1,7-enyne starting material allowed the SAR due to variation of the substituent on position 2 of the bicyclo-[3.3.0]oct-2-ene to be probed (Table 6). The tight constraints and preference for aryl groups of the LRH-1 binding site were again apparent. Although a 3-methoxyphenyl group (**18m**) was tolerated, 4-ethylphenyl (**18n**) was not, and surprisingly, neither of R = *n*Pr or *n*Bu (**18o**,**p**), both similar sizes to a phenyl group, gave active compounds. R = cyclohexyl (**18r**) gave modest binding and poor efficacy but confirms the preference for cyclohexyl over *n*-alkyl observed in the alkoxy series above (Table 4). SF-1 proved much more accommodating, consistent with the larger ligand binding pocket, although compounds with 4-ethylphenyl (**18n**) or *n*-hexyl (**18q**) substituents were not active. *n*Pr-, *n*Bu-, and *c*-hexyl-substituted compounds (**18o**,**p**,**r**) all gave similar binding and efficacy with SF-1 but distinctly poorer than compound **18a** (R = Ph). Remarkably, the 3-hydroxypropyl substituent in **18s** gave good binding and activation of LRH-1 but was inactive against SF-1, providing the only example of a highly LRH-1 selective compound. The hydroxyl group may be in a position to form a hydrogen bond with a backbone carbonyl in the N-terminal region of helix 3 of LRH-1. The inactivity of **18s** indicates this to be a very nonpolar area in SF-1.

Using alternative dihalocarbenoids in the formation of **18** allowed the biological effect of variation in the 3-substituent (Table 7) to be studied. The case R = H gave an inactive compound against both receptors, indicating that the ligand binding pocket needs to filled for binding and/or activity. Shortening the *n*-hexyl (**8a**) substituent to *n*-butyl (**18u**) gave a substantial increase in efficacy for LRH-1 without affecting SF-1 in the FRET assay. The bulky $SiMe_2Ph$ substituent gave a substantial increase in efficacy for LRH-1 and a modest decrease in both binding and efficacy for SF-1 (compare **18w** with **18a**). An *n*-octyl chain gave some reduction in binding and efficacy, particularly for LRH-1.

dx.doi.org/10.1021/jm1014296 |*J. Med. Chem.* 2011, 54, 2266–2281

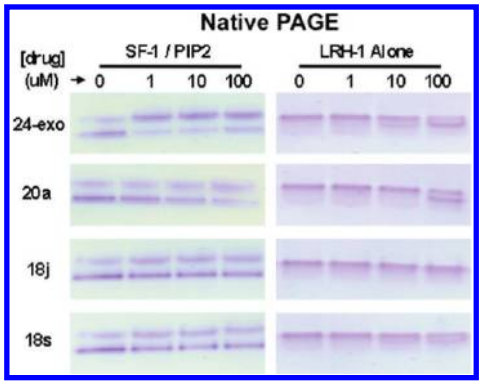

Figure 6. Differential binding to NR5A receptors. Migration of purified mouse SF-1 LBD complexed with PIP2 (SF-1/PIP2) or with human LRH-1 LBD (LRH-1 alone) in native PAGE after incubation with increasing amounts of indicated compounds. The faster migrating lower band of SF-1 LBD without compound (0) is the SF-1/PIP2 complex.

We also looked at variation in the core skeleton (Table 8). The only effect of changing the fused saturated ring from cyclopentane (in **18a**) to cyclohexane (in **19**) was reduced efficacy against SF-1. The pyrrolidine-fused systems **20a**,**b** offered the potential of improved solubility. The *N*-methyl compound **20a** was active against both receptors, although with reduced binding and efficacy, particularly against LRH-1. Given the improved solubility characteristic of **20a**, c.f., the hydrocarbons **18**, it is a useful SF-1 selective compound. Compound **20b** was LRH-1 selective but with very poor efficacy.

Finally, we examined some analogues with oxygen substitution of the cyclopentane ring. The design was driven by the crystal structure of compound **5** bound to LRH-1 described above, which indicated a polar patch (Arg-393 and His-390) in the generally hydrophobic ligand binding site (Figure 4).

We were delighted to find that introduction of a 6-*exo*-hydroxy substituent (**24**-*exo*) gave a substantial increase in both binding and efficacy against LRH-1 with more modest increases for SF-1. The *endo*-epimer of **24** showed very similar binding and efficacy against both receptors as compound **18a** lacking the oxygen substitution. Examination of Figure 4 indicates that only the *exo* alcohol is placed to interact with Arg-393 or His-390. Acylation of the *endo*-alcohol (to give **25**-*endo*) had little effect on binding to either receptor, although substantially reduced efficacy. Acylation of the *exo*-alcohol (to give **25**-*exo*) substantially reduced binding to SF-1 with little effect on LRH-1, although both showed greatly reduced efficacy.

The 7-hydroxyl-substituted systems **29**-*exo* and **29**-*endo* showed reduced binding as compared to the unsubstituted analogue **18a**, although efficacies were reasonable. Acylation of the *exo*-alcohol gave compound **30**-*exo*, which was inactive against both LRH-1 and SF-1, indicating a size limitation of this part of the binding pocket. Acylation of the endo alcohol to give **30**-*endo* was well tolerated.

Choice of Compounds as Biological Probes from the Peptide Recruitment Assay. Compound **24**-*exo* provides an excellent replacement for compound **5** as a biological tool. It has excellent stability, reasonable solubility in polar solvents, and improved binding and efficacy against both LRH-1 and SF-1. Little is lost in this FRET peptide recruitment assay by using the 1.6:1 mixture of **24**-*exo* and **24**-*endo* produced directly from the zirconium-mediated reaction, thus avoiding a tricky separation. Compounds **18o** and **18p** provide the most selective compounds

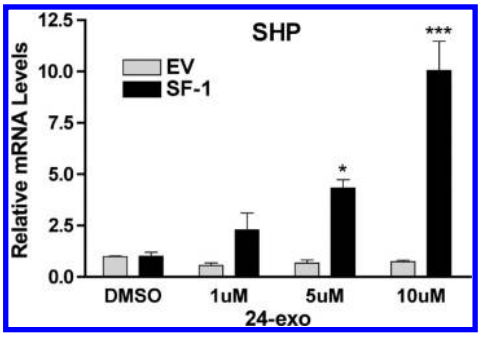

Figure 7. Dose-dependent transcriptional activation of SF-1 by **24**-*exo* in living cells. Relative mRNA levels of SHP transcript are shown in HEK293 cells stably expressing either empty vector (EV) or mouse SF-1 (SF-1) following 24 h of treatment with the indicated dosage of **24**-*exo* (μM). Expression levels are shown relative to DMSO. $^{*}p < 0.05$, and $^{***}p < 0.001$.

for SF-1, although the greater efficacy against SF-1, but still weak binding and efficacy against LRH-1 favors **18j**. The main disadvantage of all of these is their very non-polar nature, which may cause solubility problems in polar solvents, in which case pyrrolidine **20a** provides reasonable selectivity and may be preferred. Compound **18s** was unique in providing LRH-1 selectivity, although the activity was modest.

Direct Binding to Purified NR5A Receptors. Several compounds were tested for direct binding using a native gel assay, which generally maintains native protein structure and binding activities.[53] We purified both mSF-1 LBD complexed with dipalmitoyl phosphatidyl-inositol (4,5) bisphosphate (PIP2) and hLRH-1 LBD alone (no lipid added) to homogeneity as previously described,[36] then added either dimethylsulfoxide (DMSO) vehicle (0) or the indicated doses of **24**-*exo*, **20a**, **18j**, or **18s** compounds (Figure 6). These binding reactions were allowed to equilibrate for 16 h, separated by native polyacrylamide gel electrophoresis (PAGE), and SF-1 protein was visualized with Coomassie stain. The lower band in SF-1/PIP2 lanes is PIP2-dependent, while the upper band represents SF-1 no longer bound by phospholipid. Compound **24**-*exo* clearly displaces the bound PIP2 phospholipid from SF-1 almost completely at 1 μM, and similarly, **20a** can also displace PIP2 from SF-1, however, with reduced potency and efficacy (Figure 6, left panel). Compounds **18j** and **18s** do not appear competent to displace PIP2 from SF-1 LBD in this in vitro assay, even up to 100 μM.

Using hLRH-1 LBD alone that had not been complexed with any phospholipids (Figure 6, right panel), we observed a clear dose-dependent shift in hLRH-1 LBD native PAGE migration upon **24**-*exo* binding, although **20a** was nearly as efficacious binding to LRH-1, a similar shift was only observed at 100 μM. Compound **18j** does not appear competent to shift hLRH-1 LBD migration in native gels. Although not very efficacious, **18s** can consistently shift hLRH-1 LBD migration in this native gel assay, albeit with reduced potency as compared to **24**-*exo*.

Transcriptional Activation of Endogenous NR5A Target Genes. Given this direct binding data, we then asked if **24**-*exo* was capable of regulating the SF-1-mediated transcription of an endogenous target gene in living human cells. Human embryonic kidney 293 (HEK293) cells stably expressing either empty vector or SF-1 were treated with either DMSO vehicle or the indicated doses of **24**-*exo* for 24 h; each sample was subjected to real-time quantitative polymerase chain reaction (RT-qPCR) to evaluate the relative mRNA expression of the endogenous SF-1 target

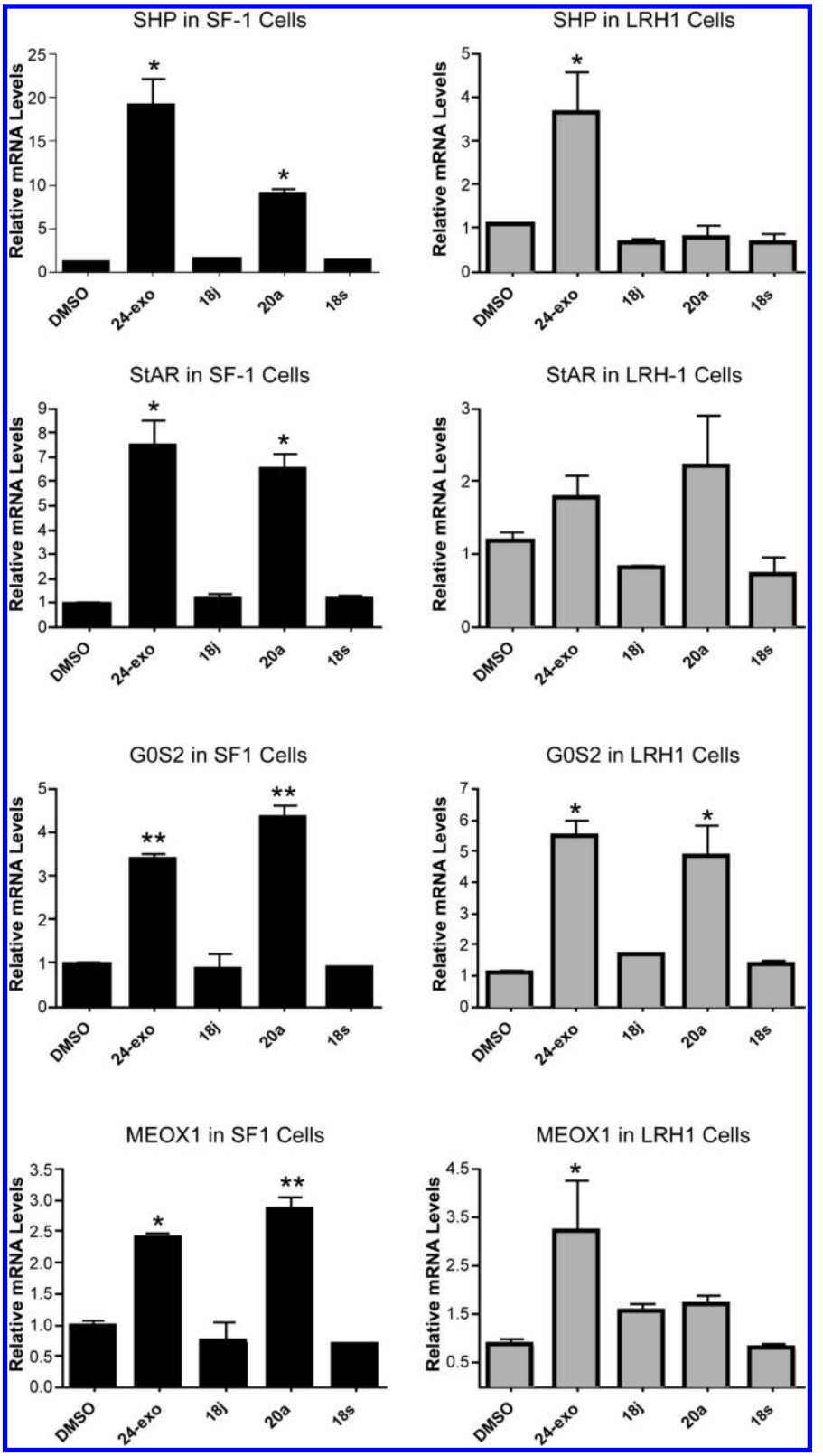

Figure 8. Differential transcriptional activation of endogenous NR5A targets in living cells. Relative mRNA expression of endogenous NR5A target genes in HEK293 cells stably expressing either mSF-1 or hLRH-1. For each gene assessed, expression levels are shown relative to DMSO following 24 h of treatment with indicated compound (10 μM). *$p < 0.05$, and **$p < 0.01$.

gene *SHP* (Figure 7). Compound **24**-*exo* induced a significant dose-dependent increase in *SHP* transcripts beginning at 5 μM; induction was dependent on the presence of SF-1 in these cells.

We next constructed a stable hLRH-1 HEK293 cell line in addition to the SF-1 line and tested each compound for activation of multiple endogenous target genes, which were previously

dx.doi.org/10.1021/jm1014296 |*J. Med. Chem.* 2011, 54, 2266–2281

identified using microarrays and gene profiling.[54] SF-1 or LRH-1 cells were treated with 10 μM of indicated compounds for 24 h, and the relative mRNA expression of each transcript was determined by RT-qPCR. SF-1 and LRH-1 protein levels were comparable in stably expressing cell lines, as determined by Western blots (data not shown). We noted that cell viability and expression of housekeeping genes appeared unchanged following treatment with compounds when compared to DMSO treatment.

Consistent with the phospholipid displacement assay, both **24**-*exo* and **20a** significantly activate SF-1-mediated transcription of the endogenous *SHP*, *StAR*, *G0S2*, and *MeOX1* target genes, while **18j** and **18s** do not (Figure 8, left panel). Also consistent with the native gel assay, selective activation of all genes by LRH-1 is observed in response to 10 μM **24**-*exo* but not with similar amounts of **18j** and **18s** (Figure 8, right panel). Interestingly, while **20a** activated LRH-1 transcription of the *StAR* and *G0S2* genes, this compound failed to activate the *SHP* and *MeOx1* genes, suggesting that when bound to **20a**, LRH-1's ability to recruit needed cofactors at all genomic targets might be compromised. Although **18j** binds LRH-1 well, it exhibits poor efficacy at these particular target genes in the HEK293 cell line, raising the possibility that a more relevant cellular or tissue context (such as liver cells) might be required for **18j** to fully activate LRH-1.

CONCLUSION

A series of 1-alkoxy- and 1-alken-2-yl-substituted bicyclo[3.3.0]oct-2-enes and related bicycles were designed, synthesized, and evaluated as agonists for the orphan NRs LRH-1 and SF-1. The study achieved its main aims: a compound (in **24**-*exo*, RJW100) with similar activity to the best of our previous agonists but with excellent stability; several compounds including **18j** (RJW102) and **20a** (RJW103) with selectivity for SF-1, although the former was inactive in in vivo studies, probably due to very poor solubility in aqueous media; and a compound **18s** (RJW101) selective for LRH-1, although further work to improve potency is needed. The precision and consistency of the SARs are notable and probably due to the rigid bicyclic core used for all of the compounds. Our preliminary cell-based studies have demonstrated that the **24**-*exo* is a consistently active agonist of SF-1 and LRH-1 target gene expression in a variety of cell lines. While the toxicity of **24**-*exo* in animals remains to remains to be determined, we are currently assessing its utility in more complex in vivo biological model systems such as in *Caenorhabditis elegans* and zebrafish, both of which express NR5A receptors. Furthermore, we expect that **24**-*exo* will be a useful chemical tool to probe the in vivo biological effects of SF-1 and LRH-1 in mammalian systems. For instance, we speculate that **24**-*exo* might eventually replace the need to virally introduce Oct-4 in an iPS assay and would thus provide one step toward achieving chemical reprogramming.

EXPERIMENTAL SECTION

Chemistry. *General.* NMR spectra were recorded on Bruker AM300 or DPX400 spectrometers in $CDCl_3$ or C_6D_6 and referenced to residual protonated solvent (^{1}H NMR) or the center peak of the deuterated solvent triplet (^{13}C NMR). Chemical shifts are reported in parts per million downfield of TMS, and the following abbreviations were used to denote coupling patterns: s, singlet; d, doublet; t, triplet; q, quartet; m, multiplet (uninterpretable or unresolved); and fs, fine splitting (resolved but unassigned small couplings). ^{13}C NMR spectra were proton decoupled and are reported as C, CH, CH_2, and CH_3, depending on the number of directly attached protons, this being determined by DEPT experiments. Assignments in NMR are only given where not easily derived from the 1D data, and systematic numbering is used. Protons described as H-a and H-b are on the *endo* and *exo* faces of the bicyclic molecules, respectively. High-resolution mass spectra (HRMS) were recorded on a VG Analytical 70-250-SE double focusing mass spectrometer using electron impact ionization (EI) (at 70 eV) or on a Bruker Apex III spectrometer using positive ion electrospray ionization. Low-resolution mass spectra (LRMS) were recorded on a VG Analytical 70-250-SE double focusing mass spectrometer (EI), a ThermoQuest TraceMS gas chromatography mass spectrometry (GCMS) [EI and CI (with ammonia as the reagent gas)], or on a VG platform quadrupole spectrometer using positive ion electrospray ionization (ESI^+). Values of m/z are reported in atomic mass units (a.m.u.) followed in parentheses by the peak intensity (relative to the base peak of 100%). IR spectra were obtained for all compounds but are not included. All compounds were >95% pure by gas chromatography performed on a Hewlett-Packard HP 6890 series GC system, using a HP-5 30 m column, with a film thickness of 0.25 μm and 0.32 mm internal diameter. The carrier gas was helium, and the flow rate was 2.7 mL min^{-1} using 100:1 split injection and an 80−275 at 25 °C/min (held at 275 °C for 4 min) temperature program with a flame ionization detector.

All organometallic reactions were carried out with dry glassware under an argon atmosphere using standard Schlenk and syringe techniques. Merck silica gel 60 (0.040−0.063 mm) was used for purification.

Unless given below, all materials were obtained from commercial sources and, if necessary, dried and distilled before use. Petrol refers to the fraction of petroleum ether that boils between 40 and 60 °C and was distilled before use. Tetrahydrofuran (THF) and diethylether used in reactions were freshly distilled from sodium/benzophenone. *n*-Butyllithium (*n*BuLi) was used as a 2.5 M solution in hexanes (Aldrich) and was stored at 4 °C.

Compounds **18b**,**h**,**k**,**m**,**o**,**r**, **19**, and **20b** are reported elsewhere.[44] The synthesis of the enyne starting materials, 1-ethyl-4-(hept-6-en-1-yn-1-yl)benzene, *N*-methyl-*N*-(phenylprop-2-ynyl)prop-2-en-1-amine, *tert*-butyldimethyl((7-phenylhept-1-en-6-yn-3-yl)oxy)silane **22**, and *tert*-butyldimethyl((7-phenylhept-1-en-6-yn-4-yl)oxy)silane **27** as well as compounds **12a**,**c**−**j**, **18c**−**g**,**i**,**l**,**n**,**p**,**q**,**t**−**w**, **25**, **29**, and **30** are given in the Supporting Information.

rac-(1S,5R)-1-Ethoxy-3-hexyl-2-phenyl-bicyclo[3.3.0]oct-2-ene (12b). To a stirred solution of *rac*-(3*S*,5*R*)-3-hexyl-2-phenyl-bicyclo[3.3.0]oct-1-en-3-ol[39] (**11**) (142 mg, 0.50 mmol) in dry THF (4 mL) at room temperature was added EtOH (0.29 mL, 5.0 mmol) followed by addition of a solution of (+)-camphorsulfonic acid (11.6 mg, 0.050 mmol) in dry THF (1 mL). The stirring was continued at the same temperature for 3.5 h after which the reaction mixture was poured onto saturated aqueous solution of $NaHCO_3$ (100 mL), and the products were extracted with Et_2O (3 × 75 mL). The combined organic phases were washed with H_2O (3 × 100 mL) and brine (100 mL). Drying over anhydrous $MgSO_4$ and filtration followed by concentration in vacuo and purification of the crude material by column chromatography on Al_2O_3 (basic, grade III) with 2.5% Et_2O in petrol as the eluent gave the title compound as a yellow oil (0.108 g, 69%). ^{1}H NMR (400 MHz, $CDCl_3$): δ 7.27−7.13 (5H, m), 3.40 (1H, m), 3.26 (1H, m), 2.65 (1H, dd, J = 17.1, 8.3 Hz, H−4b), 2.45−2.37 (1H, m, H−5), 2.14−2.08 (2H, m), 2.06−1.93 (2H, m), 1.66−1.49 (3H, m), 1.44−1.29 (3H, m), 1.24−1.10 (10H, m), 0.77 (3H, t, J = 6.8 Hz, CH_3). ^{13}C NMR (100.5 MHz, $CDCl_3$): δ 145.51 (C), 137.28 (C), 136.09 (C), 129.21 (CH), 128.10 (CH), 126.59 (CH), 103.39 (C), 58.40 (CH_2), 42.99 (CH), 42.15 (CH_2), 37.89 (CH_2), 35.83 (CH_2), 31.81 (CH_2), 29.91 (CH_2), 29.43 (CH_2), 28.25 (CH_2), 25.40 (CH_2), 22.77 (CH_2), 15.98 (CH_3), 14.21 (CH_3). LRMS (EI) m/z = 312 ([M]$^+$, 93%), 283 (100%), 195 (59%). HRMS (EI) found, [M]$^+$, 312.2458. $C_{22}H_{32}O$ requires, 312.2453.

General Procedure. To a solution of Cp_2ZrCl_2 (0.293 g, 1.0 mmol) in dry THF (5 mL) cooled to −78 °C was added *n*BuLi (0.80 mL of a 2.5 M solution in hexanes, 2.0 mmol) dropwise (over ∼2 min). After 25 min, a solution of the appropriate enyne (1.0 mmol) in dry THF (3 mL) was added dropwise. After 30 min at −78 °C, the reaction mixture was allowed to warm to room temperature and continued to stir for 2−3 h. After the reaction mixture was recooled to −78 °C, a solution of the appropriate 1,1-dihalo alkane (1.1 mmol) in dry THF (1 mL) was added followed by dropwise addition of LDA (0.64 mL of a 1.8 M solution, 1.15 mmol). The reaction mixture was stirred at −78 °C for 15 min before dropwise addition of the corresponding lithium acetylide. [Lithium acetylide was freshly prepared from alkyne (3.0 mmol) in dry THF (3 mL) and *n*BuLi (1.2 mL of a 2.5 M solution in hexanes, 3.0 mmol) at −5 °C over 15 min]. The stirring was continued for 0.5−1 h during which the reaction mixture was allowed to warm to −55 °C before addition of MeOH (10 mL) and saturated aqueous solution of $NaHCO_3$ (10 mL). The whole mixture was allowed to warm to room temperature and left stirring for 12−16 h. The mixture then was poured onto H_2O (100 mL), and the products were extracted with Et_2O (3 × 75 mL). The combined organic phases were washed with H_2O (3 × 100 mL) and brine (100 mL). Drying over anhydrous $MgSO_4$ and filtration followed by concentration in vacuo gave the crude products mostly as yellow oils.

rac-(1R,5R)-3-Hexyl-2-phenyl-1-(1-phenylvinyl)-bicyclo[3.3.0]oct-2-ene (18a). General procedure was used with 1-(hept-6-en-1-ynyl)benzene, 1,1-dibromoheptane, and 1-ethynylbenzene as components. Purification of the crude material by column chromatography on SiO_2 (230−400 mesh) with hexanes as the eluent gave the title compound as a pale yellow oil (0.318 g, 86%). ^{1}H NMR (300 MHz, $CDCl_3$): δ 7.35−7.24 (10H, m), 5.04 (1H, d, J = 1.6 Hz, C=CH_2), 5.02 (1H, d, J = 1.6 Hz, C=CH_2), 2.43 (1H, tdd, J = 8.6, 3.2, 1.4 Hz, H−5), 2.34 (1H, fs ddd, J = 16.2, 8.4, 1.0 Hz, H−4b), 2.12−1.97 (3H, m), 1.85 (1H, dtd, J = 12.2, 9.7, 6.8 Hz), 1.68 (2H, m), 1.62−1.52 (3H, m), 1.43−1.21 (8H, m), 0.88 (3H, t, J = 6.8 Hz, CH_3). ^{13}C NMR (75 MHz, $CDCl_3$): δ 155.39 (*C*=CH_2), 144.40 (C), 142.48 (C), 138.95 (C), 137.98 (C), 129.69 (2CH), 127.93 (2CH), 127.55 (2CH), 127.52 (2CH), 126.47 (CH), 126.33 (CH), 114.45 (C=*CH*$_2$), 70.16 (C−1), 45.71 (CH−5), 43.83 (CH_2), 36.33 (CH_2), 35.64 (CH_2), 31.70 (CH_2), 29.89 (CH_2), 29.41 (CH_2), 27.87 (CH_2), 25.60 (CH_2), 22.60 (CH_2), 14.06 (CH_3). LRMS (EI) m/z: 370 ([M]$^{+\cdot}$, 100%), 299 (35%), 267 (85%). HRMS (EI) found, [M]$^+$, 370.2655. $C_{26}H_{34}$ requires, 370.2661.

rac-(1R,5R)-1-(Hex-1-en-2-yl)-3-hexyl-2-phenyl-bicyclo[3.3.0]oct-2-ene (18j). General procedure was used with 1-(hept-6-en-1-ynyl)benzene, 1,1-dibromoheptane, and 1-hexyne as components. Purification of the crude material by column chromatography on SiO_2 (230−400 mesh) with hexanes as the eluent gave the title compound as a pale yellow oil (0.263 g, 75%). ^{1}H NMR (300 MHz, $CDCl_3$): δ 7.29−7.17 (3H, m), 7.06−7.02 (2H, m), 4.81 (1H, q, J = 1.4 Hz, C=CH_2), 4.79 (1H, q, J = 1.4 Hz, C=CH_2), 2.84 (1H, fs dd, J = 16.8, 8.4 Hz, H−4b), 2.43 (1H, dddd, J = 9.7, 8.4, 3.2, 1.6 Hz, H−5), 2.21−2.01 (5H, m), 1.88 (1H, dtd, J = 12.0, 9.4, 7.0 Hz, H−6), 1.70 (1H, m), 1.60−1.48 (6H, m), 1.45−1.33 (4H, m), 1.30−1.21 (6H, m), 0.95 (3H, t, J = 7.2 Hz, CH_3), 0.86 (3H, t, J = 6.9 Hz, CH_3). ^{13}C NMR (75 MHz, $CDCl_3$): δ 154.57 (*C*=CH_2), 141.21 (C), 139.63 (C), 138.04 (C), 129.40 (2CH), 127.42 (2CH), 126.11 (CH), 107.27 (C=*CH*$_2$), 71.24 (C−1), 45.53 (CH−5), 44.33 (CH_2), 36.67 (CH_2), 33.84 (CH_2), 32.05 (CH_2), 31.68 (CH_2), 30.75 (CH_2), 29.59 (CH_2), 29.13 (CH_2), 28.06 (CH_2), 25.70 (CH_2), 23.05 (CH_2), 22.61 (CH_2), 14.15 (CH_3), 14.04 (CH_3). LRMS (EI) m/z: 350 ([M]$^{+\cdot}$, 57%), 307 (26%), 293 (100%). HRMS (EI) found, [M]$^+$, 350.2979. $C_{26}H_{38}$ requires, 350.2974.

r a c -(1R,5R)-3-Hexyl-1-(phenylvinyl)-2-(propan-3-ol)-bicyclo[3.3.0]oct-2-ene (18s). General procedure was used with *tert*-butyl(dec-9-en-4-yn-1-yloxy)dimethylsilane, 1,1-dibromoheptane, and 1-ethynylbenzene as components with the exception that the reaction was carried out on 2.0 mmol scale. Crude product from the three component coupling was purified by flash column chromatography on silica, and then, the TBDMS group was removed with TBAF [2.0 mL of a 1.0 M solution in THF (2.0 mmol) in dry THF (8.0 mL) at room temperature for 20 h]. Purification of the crude material by column chromatography on SiO_2 (230−400 mesh) with hexanes as the eluent gave the title compound as a yellow oil (0.430 g, 61% over two steps). ^{1}H NMR (400 MHz, $CDCl_3$): δ 7.24−7.16 (5H, m), 5.15 (1H, d, J = 1.8 Hz, C=CH_2), 4.98 (1H, d, J = 1.8 Hz, C=CH_2), 3.65 (2H, q, J = 6.5 Hz, CH_2OH), 2.34 (1H, tt, J = 9.0, 2.0 Hz, H−5), 2.24 (1H, dd, J = 16.0, 9.0 Hz, H−4b), 2.13−2.02 (4H, m), 1.87−1.61 (6H, m), 1.59−1.52 (1H, m), 1.48−1.38 (1H, m), 1.37−1.26 (10H, m), 0.91 (3H, t, J = 6.9 Hz, CH_3). ^{13}C NMR (100.5 MHz, $CDCl_3$): δ 155.95 (*C*=CH_2), 144.36 (C), 139.80 (C), 136.21 (C), 127.83 (2CH), 127.37 (2CH), 126.33 (CH), 113.26 (C=*CH*$_2$), 70.38 (C−1), 63.62 (*CH*$_2$OH), 43.99 (CH−5), 43.80 (CH_2−4), 36.55 (CH_2), 36.05 (CH_2), 33.45 (CH_2), 31.84 (CH_2), 29.52 (CH_2), 29.27 (CH_2), 27.73 (CH_2), 25.34 (CH_2), 22.65 (CH_2), 22.54 (CH_2), 14.10 (CH_3). LRMS (CI) m/z: 353 ([M + H]$^+$, 100%), 249 (37%). HRMS (EI) found, [M]$^+$, 352.2767. $C_{25}H_{36}O$ requires, 352.2766.

rac-(1S,5R)-3-Hexyl-2-phenyl-1-(phenylvinyl)-7-methylaza-bicyclo[3.3.0]oct-2-ene (20a). General procedure was used with *N*-methyl-*N*-(phenylprop-2-ynyl)prop-2-en-1-amine, 1,1-dibromoheptane, and 1-ethynylbenzene as components. Purification of the crude material by column chromatography on Al_2O_3 (basic, grade III) with 2.5% of Et_2O in hexanes as the eluent gave the title compound as a pale yellow oil (0.240 g, 62%). ^{1}H NMR (400 MHz, $CDCl_3$): δ 7.38−7.25 (10H, m), 5.10 (1H, d, J = 1.1 Hz, C=CH_2), 4.93 (1H, d, J = 1.1 Hz, C=CH_2), 2.69 (1H, d, J = 9.4 Hz, H−8), 2.68 (1H, dd, J = 8.4, 4.0 Hz, H−6), 2.63 (1H, d, J = 9.4 Hz, H−8), 2.63 (1H, tdd, J = 7.9, 4.0, 2.0 H−5), 2.50 (1H, fs dd, J = 16.8, 8.8, Hz, H−4b), 2.45 (1H, dd, J = 8.4, 4.0 Hz, H−6), 2.31 (3H, s, N−CH_3), 2.15 (1H, dd, J = 16.8, 1.7, Hz, H−4a), 2.12−2.08 (2H, m, C−3−*CH*$_2$), 1.45−1.34 (2H, m), 1.32−1.22 (6H, m,), 0.89 (3H, t, J = 7.0 Hz, CH_3). ^{13}C NMR (100.5 MHz, $CDCl_3$): δ 153.64 (*C*=CH_2), 143.66 (C), 141.53 (C), 139.52 (C), 137.54 (C), 129.89 (2CH), 127.73 (2CH), 127.65 (2CH), 127.57 (2CH), 126.71 (CH), 126.46 (CH), 114.98 (C=*CH*$_2$), 70.11 (C−1), 65.77 ($2CH_2$−6 + 8), 46.35 (CH−5), 42.73 (N−CH_3), 41.98 (CH_2−4), 31.67 (CH_2), 29.81 (CH_2), 29.39 (C−3−*CH*$_2$), 27.72 (CH_2), 22.58 (CH_2), 14.06 (CH_3). LRMS (ESI$^+$) m/z: 386 ([M + H]$^+$, 100%). HRMS (ESI$^+$) found, [M + H]$^+$, 386.2832. [$C_{28}H_{36}N$]$^+$ requires, 386.2842.

rac-(1R,5R,6R)-3-Hexyl-6-hydroxy-2-phenyl-1-(phenylvinyl)-bicyclo[3.3.0]oct-2-ene (24-exo) and rac-(1R,5R,6S)-3-Hexyl-6-hydroxy-2-phenyl-1-(phenylvinyl)-bicyclo[3.3.0]oct-2-ene (24-endo). To a solution of Cp_2ZrCl_2 (1.465 g, 5.0 mmol) in dry THF (25 mL) cooled to −78 °C was added *n*BuLi (4.0 mL of a 2.5 M solution in hexanes, 10.0 mmol) dropwise. After 20 min, a solution of *tert*-butyldimethyl((7-phenylhept-1-en-6-yn-3-yl)oxy)silane (1.50 g, 5.0 mmol) in dry THF (15 mL) was added dropwise. After 30 min at −78 °C, the reaction mixture was allowed to warm to room temperature and continued to stir for 3 h. After the reaction mixture was recooled to −78 °C, a solution of 1,1-dibromoheptane (1.42 g, 5.5 mmol) in dry THF (5 mL) was added followed by dropwise addition of LDA (3.06 mL of a 1.8 M solution, 5.5 mmol). The reaction mixture was stirred at −78 °C for 15 min before dropwise addition of lithium phenylacetylide solution [freshly prepared from phenylacetylene (1.65 mL, 15.0 mmol) in dry THF (15 mL) and *n*BuLi (6.0 mL of a 2.5 M solution in hexanes, 15.0 mmol) at −10 °C over 15 min]. The stirring was continued for 45 min during which the reaction mixture was allowed to warm to −55 °C before addition of MeOH (30 mL) and saturated aqueous solution of $NaHCO_3$ (30 mL). The mixture was allowed to warm to room temperature and left stirring for 5 h before pouring onto H_2O (200 mL) and extracting the products into Et_2O (3 × 200 mL). The combined organic phases were washed with

H_2O (3 × 300 mL) and brine (300 mL). Drying over anhydrous $MgSO_4$ and filtration followed by concentration in vacuo gave the crude product as a yellow oil. Purification by flash chromatography on SiO_2 with 2.5% of Et_2O in hexanes furnished the TBDMS protected alcohols **23** (1.6:1 exo:endo) as a yellow oil (2.20 g, 88%).

The TBDMS-protected alcohols **23** (2.20 g, 4.40 mmol) were dissolved in dry THF (44 mL) followed by addition of TBAF (17.60 of 1.0 M solution in THF), and the reaction mixture was stirred at room temperature for 20 h. Then, the mixture was poured onto H_2O (200 mL) and extracted with Et_2O (2 × 150 mL). The organic phases were washed with H_2O (3 × 200 mL) and brine (1 × 200 mL) and dried over $MgSO_4$. Concentration in vacuo, followed by separation by column chromatography on Al_2O_3 (basic, grade III) and 2.5% EtOAc in hexanes as the eluent gave the partly separated isomers: 0.277 g of pure **24**-*endo* (14%), 0.650 g of mixed fractions (33%), and 0.556 g of pure **24**-*exo* (29%), for a combined yield of 1.483 g (76%). Further chromatography of the mixed fractions allowed additional pure **24**-*exo* and **24**-*endo* to be isolated. Compound **24**-*exo*: ^{1}H NMR (300 MHz, $CDCl_3$): δ 7.37−7.19 (10H, m), 5.08 (1H, d, J = 1.5 Hz, C=CH_2), 5.00 (1H, d, J = 1.5 Hz, C=CH_2), 3.96 (1H, br s, H−6), 2.39 (1H, fs dd, J = 16.2, 9.6 Hz, H−4b), 2.30 (1H, fs d, J = 9.6 Hz, H−5), 2.15−2.0 (4H, m), 1.79−1.67 (3H, m), 1.38−1.20 (9H, m), 0.87 (3H, t, J = 6.8 Hz, CH_3). ^{13}C NMR (75 MHz, $CDCl_3$): δ 154.69 (*C*=CH_2), 144.21 (C), 141.19 (C), 139.17 (C), 137.43 (C), 129.73 (2CH), 127.78 (2CH), 127.72 (2CH), 127.62 (2CH), 126.66 (CH), 126.59 (CH), 114.99 (C=CH_2), 82.10 (CH−6), 69.40 (C−1), 55.92 (CH−5), 40.29 (CH_2), 34.04 (CH_2), 32.13 (CH_2), 31.66 (CH_2), 29.73 (CH_2), 29.37 (CH_2), 27.83 (CH_2), 22.58 (CH_2), 14.06 (CH_3). LRMS (EI) m/z: 386 ($[M]^{+\bullet}$, 36%), 283 (21%), 283 (100%). HRMS (EI) found, $[M]^+$, 386.2611. $C_{28}H_{34}O$ requires, 386.2610. Compound **24**-*endo*: ^{1}H NMR (300 MHz, $CDCl_3$): δ 7.35−7.21 (10H, m), 5.075 (1H, d, J = 1.5 Hz, C=CH_2), 4.96 (1H, d, J = 1.5 Hz, C=CH_2), 4.19 (1H, ddd, J = 9.1, 8.5, 5.5 Hz, H−6), 2.63 (1H, fs dd, J = 17.2, 2.1 Hz, H−4a), 2.50 (1H, fs td, J = 8.5, 2.1 Hz, H−5), 2.17−2.01 (3H, m), 1.86 (1H, ddt, J = 10.4, 5.5, 4.4 Hz, H−7b), 1.74−1.70 (2H, m), 1.57 (1H, ddd, J = 10.4, 9.1, 8.1 Hz, H−7a), 1.50−1.35 (2H, m), 1.29−1.24 (7H, m), 0.87 (3H, t, J = 6.8 Hz, CH_3). ^{13}C NMR (75 MHz, $CDCl_3$): δ 154.86 (*C*=CH_2), 144.00 (C), 143.28 (C), 139.37 (C), 137.06 (C), 129.82 (2CH), 127.78 (2CH), 127.70 (2CH), 127.61 (2CH), 126.70 (CH), 126.56 (CH), 114.88 (C=CH_2), 74.55 (CH−6), 68.83 (C−1), 49.19 (CH−5), 33.77 (CH_2), 33.49 (CH_2), 31.83 (CH_2), 31.66 (CH_2), 29.89 (CH_2), 29.47 (CH_2), 27.93 (CH_2), 22.60 (CH_2), 14.06 (CH_3). LRMS (EI) m/z: 386 ($[M]^{+\bullet}$, 12%), 368 (17%), 283 (69%). HRMS (EI) found, $[M]^+$, 386.2600. $C_{28}H_{34}O$ requires, 386.2610.

Biology Experimental. *Transcriptional Assays.* Stable cell lines expressing either N-terminal 3XFlag-tagged mouse SF-1 or human LRH-1 were generated with the T-Rex Flip-In system in the HEK293 T-Rex cell line (Invitrogen). Expression and tetracycline (Tet) inducibility were verified by Western blot analysis using an anti-3XFlag M2 monoclonal antibody (Sigma). For all transcriptional assays, compounds dissolved in DMSO were added for 16 h after initial addition of 100 ng/mL Tet or EtOH vehicle control. Low levels of transduced SF-1 and LRH-1 were observed in cell lines before the addition of Tet, most likely due to stochastic "leakiness" of the TET-transcriptional repressor, as often observed. Messenger RNA transcript abundance relative to the cyclophilin housekeeping gene is shown, with DMSO control set equal to 1. All transcripts were analyzed by quantitative PCR using the following sets of validated primers:

hCyclophilinf	TTTCATCTGCACTGCCAAGA
hCyclophilinr	TTGCCAAACACCACATGCT
hSHPf	GCTTAGCCCCAAGGAATATGC
hSHPr	TTGGAGGCCTGGCACATC
hStARf	CCCATGGAGAGGCTCTATGAA
hStARr	GTTCCACTCCCCCATTGCT
hMEOX1f	GGCGGAGAAAGGAGAGTTCA
hMEOX1r	TCCTTGCGGGCTTTGCT
hG0S2f	CAGAGAAACCGCTGACATCTAGAA
hG0S2r	CAGCAAAACTCAATCCCAAACTC

Protein Purification and PI(4,5)P2 Displacement. Details of the SF-1 LBD construct, purification, and PI(4,5)P2 exchange have been previously described.[35b,36] For compound displacement assays, 2.0 μL of serially diluted compounds in DMSO were dosed into 48.0 μL of crystallography pure 1.0 μM mSF-1 LBD/PI(4,5)P2 complexes, in 20 mM 4-(2-hydroxyethyl)-1-piperazineethanesulfonic acid (HEPES) (8.0) and 5 mM $MgCl_2$, for 2 h at 37 °C. This entire reaction was then separated by native PAGE on precast 4−16% gradient Bis/Tris-buffered gels (Invitrogen), which maintains SF-1LBD/PI(4,5,)P2 association. Gels were then stained with Coomassie brilliant blue to visualize compound-induced changes in the native gel migration pattern of SF-1 LBD/PI(4,5)P2.

Crystallography. Purification of human LRH-1 is as described previously.[35b] Endogenous phospholipids were replaced with GR8470 (compound **5**) using liposome-mediated exchange as described[35b] with the exception that liposomes were composed of 1,2-ditetracosanoyl-*sn*-glycero-3-phosphocholine (PC24) (Avanti Polar Lipids). Briefly, GR8470 in DMSO was added to PC24 in water to a final concentration of 0.8 mM and was mixed with an equal volume of 8 mg/mL LRH-1, giving a final ligand:protein ratio of 3. Exchange was monitored by purifying the LRH-1/ligand complex on a PD10 size exclusion column and determining the complex molecular weight by mass spectroscopy as described.[35b] By this method, exchange did not improve beyond 5 days. Purified LRH-1 was then mixed with TIF2 peptide in a 1:2 molar ratio and concentrated to 6−8 mg/mL for crystallization trials.

Crystals of the complex were obtained in 0.2 M ammonium sulfate, 0.1 M sodium acetate trihydrate, pH 4.6, and 25% w/v polyethylene glycol 4000 and were quickly dunked into the same buffer with 12% glycerol and 12% ethylene glycol prior to freezing in liquid nitrogen.

Data were collected at beamline 17ID (IMCA CAT) at the Advanced Photon Source at Argonne National Laboratories using an ADSC Q210. Images were integrated and scaled using HKL2000. The complex crystallized in the space group $P2_1$ with unit cell constants of A = 52.7, B = 89.0, C = 65.4, and β = 101.7, with two complexes per asymmetric unit. The structure was solved by molecular replacement using the apo LRH-1 structure (1YOK) as a search model. The model was refined against 1.75 Å data using Refmac5[55] and rebuilt using Coot.[56] The model was refined to a final R = 18.7 and R_{free} = 21.4 and contained two copies of LRH-1 LBD, two copies of TIF2 peptide, two copies GR8470, one glycerol molecule, three ethylene glycol molecules, and 305 water molecules. The bond length and angle root-mean-square deviation from ideality are 0.007 Å and 1.098°, respectively.

■ ASSOCIATED CONTENT

Supporting Information. Details of the synthesis and characterization of enyne cyclization precursors and compounds **12a,c−j**, **18c−g,i,l,n,p,q,t−w**, **25**-*exo*, **25**-*endo*, **29**-*exo*, **29**-*endo*, **30**-*exo*, and **30**-*endo* and statistical analysis of the peptide recruitment assay results. This material is available free of charge via the Internet at http://pubs.acs.org.

Accession Codes

The X-ray coordinates of compound **5** bound to LRH-1 LBD have been deposited in the Protein Data Bank with accession number 3PLZ.

AUTHOR INFORMATION

Corresponding Author
*Tel: 23 80592777. E-mail: rjw1@soton.ac.uk.

ACKNOWLEDGMENT

R.J.W., J.S., and S.D. thank GlaxoSmithKline for generous funding.

ABBREVIATIONS USED

APC, allophycocyanin; NR, nuclear receptor; SF-1, steroidogenic factor-1 (NR5A1); LRH-1, liver receptor homologue-1 (NR5A2); DBD, DNA binding domain; LBD, ligand binding domain; SHP, small/short heterodimer partner (NR01B); DAX-1, dosage-sensitive sex reversal adrenal hypoplasia critical region on chromosome Xgene 1) (NR0B2); FXR, farnesoid X receptor; PPAR, peroxisome proliferator-activated receptor; PC, phosphatidylcholine; LDA, lithium diisopropylamide; LiTMP, lithium 2,2,6,6-tetramethylpiperidide; TBAF, tetrabutylammonium fluoride; TBDMS, *t*Bu-Me_2Si; HMPA, hexamethylphosphoramide; DMAP, 4-dimethylaminopyridine; TR, time-resolved; FRET, fluorescence resonance energy transfer; RT-qPCR, real-time quantitative polymerase chain reaction; HEK293, human embryonic kidney 293; RE, relative efficacy; DMSO, dimethylsulfoxide; HEPES, 4-(2-hydroxyethyl)-1-piperazineethanesulfonic acid; iPS, induced pluripotent stem cell; PAGE, polyacrylamide gel electrophoresis; DOX, doxycycline; Tet, tetracycline; PIP2, dipalmitoyl phosphatidyl-inositol (4,5) bisphosphate; G0S2, G0/G1 switch regulatory protein 2; MeOX1, mesenchyme homeobox protein 1; StAR, steroidogenic acute regulatory protein; HRMS, high-resolution mass spectra; EI, electron impact ionization; CI, chemical ionization; LRMS, low-resolution mass spectra; GC-MS, gas chromatography—mass spectrometry; NMR, nuclear magnetic resonance; THF, tetrahydrofuran; PC24, 1,2-ditetracosanoyl-*sn*-glycero-3-phosphocholine; TIF-2, transcriptional intermediary factor 2

REFERENCES

(1) Russell, D. W.; Mangelsdorf, D. J. *Nuclear Receptors*, 1st ed.; Academic Press Inc.: London, 2003; Vol. 363.

(2) (a) Schweitzer, A.; Knauer, S. K.; Stauber, R. H. Therapeutic potential of nuclear receptors. *Expert Opin. Ther. Pat.* **2008**, *18*, 861–888. (b) Moore, J. T.; Collins, J. L.; Pearce, K. H. The nuclear receptor superfamily and drug discovery. *ChemMedChem* **2006**, *1*, 504–523. (c) Shi, Y. H. Orphan nuclear receptors in drug discovery. *Drug Discovery Today* **2007**, *12*, 440–445. (d) Mukherjee, S.; Mani, S. Orphan nuclear receptors as targets for drug development. *Pharm. Res.* **2010**, *27*, 1439–1468.

(3) Overington, J. P.; Al-Lazikani, B.; Hopkins, A. L. Opinion - How many drug targets are there?. *Nature Rev. Drug Discovery* **2006**, *5*, 993–996.

(4) Benoit, G.; Cooney, A.; Giguere, V.; Ingraham, H.; Lazar, M.; Muscat, G.; Perlmann, T.; Renaud, J. P.; Schwabe, J.; Sladek, F.; Tsai, M. J.; Laudet, V. International Union of Pharmacology. LXVI. Orphan nuclear receptors. *Pharmacol. Rev.* **2006**, *58*, 798–836.

(5) (a) Willson, T. M.; Jones, S. A.; Moore, J. T.; Kliewer, S. A. Chemical genomics: Functional analysis of orphan nuclear receptors in the regulation of bile acid metabolism. *Med. Res. Rev.* **2001**, *21*, 513–522. (b) Hummasti, S.; Tontonoz, P. Adopting new orphans into the family of metabolic regulators. *Mol. Endocrinol.* **2008**, *22*, 1743–1753. (c) Schulman, I. G.; Heyman, R. A. The flip side: Identifying small molecule regulators of nuclear receptors. *Chem. Biol.* **2004**, *11*, 639–646.

(6) Kliewer, S. A.; Lehmann, J. M.; Willson, T. M. Orphan nuclear receptors: Shifting endocrinology into reverse. *Science* **1999**, *284*, 757–760.

(7) Parks, D. J.; Blanchard, S. G.; Bledsoe, R. K.; Chandra, G.; Consler, T. G.; Kliewer, S. A.; Stimmel, J. B.; Willson, T. M.; Zavacki, A. M.; Moore, D. D.; Lehmann, J. M. Bile acids: Natural ligands for an orphan nuclear receptor. *Science* **1999**, *284*, 1365–1368.

(8) Lee, C. H.; Olson, P.; Evans, R. M. Minireview: Lipid metabolism, metabolic diseases, and peroxisome proliferator-activated receptors. *Endocrinology* **2003**, *144*, 2201–2207.

(9) (a) Val, P.; Lefrancois-Martinez, A.-M.; Veyssiere, G.; Martinez, A. SF-1 a key player in the development and differentiation of steroidogenic tissues. *Nucl. Recept.* **2003**, *1*, 8. (b) Schimmer, B. P.; White, P. C. Minireview: Steroidogenic fctor 1: Its roles in differentiation development and disease. *Mol. Endocrinol.* **2010**, *24*, 1322–1337.

(10) Fayard, E.; Auwerx, J.; Schoonjans, K. LRH-1: An orphan nuclear receptor involved in development, metabolism and steroidogenesis. *Trends Cell Biol.* **2004**, *14*, 250–260.

(11) Hoivik, E. A.; Lewis, A. E.; Aumo, L.; Bakke, M. Molecular aspects of steroidogenic factor 1 (SF-1). *Mol. Cell. Endocrinol.* **2010**, *315*, 27–39.

(12) Lin, L.; Achermann, J. C. Steroidogenic Factor-1 (SF-1, Ad4BP, NR5A1) and Disorders of Testis Development. *Sex. Dev.* **2008**, *2*, 200–209.

(13) (a) Husebye, E. S.; Lovas, K. Immunology of Addison's Disease and Premature Ovarian Failure. *Endocrinol. Metab. Clin. North Am.* **2009**, *38*, 389–405. (b) Lourenco, D.; Brauner, R.; Lin, L.; De Perdigo, A.; Weryha, G.; Muresan, M.; Boudjenah, R.; Guerra, G.; Maciel-Guerra, A. T.; Achermann, J. C.; McElreavey, K.; Bashamboo, A. Mutations in NR5A1 Associated with Ovarian Insufficiency. *N. Engl. J. Med.* **2009**, *360*, 1200–1210.

(14) Doghman, M.; Cazareth, J.; Douguet, D.; Madoux, F.; Hodder, P.; Lalli, E. Inhibition of Adrenocortical Carcinoma Cell Proliferation by Steroidogenic Factor-1 Inverse Agonists. *J. Clin. Endocrinol. Metab.* **2009**, *94*, 2178–2183.

(15) (a) Bulun, S. E.; Utsunomiya, H.; Lin, Z. H.; Yin, P.; Cheng, Y. H.; Pavone, M. E.; Tokunaga, H.; Trukhacheva, E.; Attar, E.; Gurates, B.; Milad, M. P.; Confino, E.; Su, E.; Reierstad, S.; Xue, Q. Steroidogenic factor-1 and endometriosis. *Mol. Cell. Endocrinol.* **2009**, *300*, 104–108. (b) Dube, C.; Bergeron, F.; Vaillant, M. J.; Robert, N. M.; Brousseau, C.; Tremblay, J. J. The nuclear receptors SF1 and LRH1 are expressed in endometrial cancer cells and regulate steroidogenic gene transcription by cooperating with AP-1 factors. *Cancer Lett.* **2009**, *275*, 127–138. (c) Lin, B. C.; Suzawa, M.; Blind, R. D.; Tobias, S. C.; Bulun, S. E.; Scanlan, T. S.; Ingraham, H. A. Stimulating the GPR30 Estrogen Receptor with a Novel Tamoxifen Analogue Activates SF-1 and Promotes Endometrial Cell Proliferation. *Cancer Res.* **2009**, *69*, 5415–5423.

(16) (a) Kim, K. W.; Zhao, L. P.; Parker, K. L. Central nervous system-specific knockout of steroidogenic factor 1. *Mol. Cell. Endocrinol.* **2009**, *300*, 132–136. (b) Zhao, L.; Kim, K. W.; Ikeda, Y.; Anderson, K. K.; Beck, L.; Chase, S.; Tobet, S. A.; Parker, K. L. Central nervous system-specific knockout of steroidogenic factor 1 results in increased anxiety-like behavior. *Mol. Endocrinol.* **2008**, *22*, 1403–1415.

(17) Gu, P.; Goodwin, B.; Chung, A. C. K.; Xu, X.; Wheeler, D. A.; Price, R. R.; Galardi, C.; Li, P.; Latour, A. M.; Koller, B. H.; Gossen, J.; Kliewer, S. A.; Cooney, A. J. Orphan nuclear receptor LRH-1 is required to maintain Oct4 expression at the epiblast stage of embryonic development. *Mol. Cell. Biol.* **2005**, *25*, 3492–3505.

(18) Lee, Y.-K.; Moore, D. D. Liver receptor homolog-1, an emerging metabolic modulator. *Front. Biosci.* **2008**, *13*, 5950–5958.

(19) Lee, Y. K.; Schmidt, D. R.; Cummins, C. L.; Choi, M.; Peng, L.; Zhang, Y.; Goodwin, B.; Hammer, R. E.; Mangelsdorf, D. J.; Kliewer, S. A. Liver receptor homolog-1 regulates bile acid homeostasis but is not essential for feedback regulation of bile acid synthesis. *Mol. Endocrinol.* **2008**, *22*, 1345–1356.

(20) Venteclef, N.; Smith, J. C.; Goodwin, B.; Delerive, P. Liver receptor homolog 1 is a negative regulator of the hepatic acute-phase response. *Mol. Cell. Biol.* **2006**, *26*, 6799–6807.

(21) Goodwin, B. J.; Stewart, E. L.; Brown, P. J.; Delerive, P. Liver receptor homolog-1 (LRH1) activators as medicaments for diseases or conditions caused by low plasma apoA-1 levels. WO 2005082344, 2005.

(22) Zollner, G.; Trauner, M. Nuclear receptors as therapeutic targets in cholestatic liver diseases. *Br. J. Pharmacol.* **2009**, *156*, 7–27.

(23) Santen, R. J.; Brodie, H.; Simpson, E. R.; Siiteri, P. K.; Brodie, A. History of Aromatase: Saga of an Important Biological Mediator and Therapeutic Target. *Endocr. Rev.* **2009**, *30*, 343–375.

(24) (a) Zhou, J.; Suzuki, T.; Kovacic, A.; Saito, R.; Miki, Y.; Ishida, T.; Moriya, T.; Simpson, E. R.; Sasano, H.; Clyne, C. D. Interactions between prostaglandin E-2, liver receptor homologue-1, and aromatase in breast cancer. *Cancer Res.* **2005**, *65*, 657–663. (b) Annicotte, J. S.; Chavey, C.; Servant, N.; Teyssier, J.; Bardin, A.; Licznar, A.; Badia, E.; Pujol, P.; Vignon, F.; Maudelonde, T.; Lazennec, G.; Cavailles, V.; Fajas, L. The nuclear receptor liver receptor homolog-1 is an estrogen receptor target gene. *Oncogene* **2005**, *24*, 8167–8175. (c) Chen, D.; Reierstad, S.; Lu, M. L.; Lin, Z. H.; Ishikawa, H.; Bulun, S. E. Regulation of breast cancer-associated aromatase promoters. *Cancer Lett.* **2009**, *273*, 15–27. (d) Simpson, E. R.; McDonnell, D. P.; Kovacic, A.; Clyne, C. D.; Safi, R. Regulation of aromatase expression in the breast by LRH-1: A new potential target for breast cancer therapy. *Breast Cancer Res. Treat.* **2005**, *94*, S236–S236. (e) Miki, Y.; Clyne, C. D.; Suzuki, T.; Moriya, T.; Shibuya, R.; Nakamura, Y.; Ishida, T.; Yabuki, N.; Kitada, K.; Hayashi, S.-i.; Sasano, H. Immunolocalization of liver receptor homologue-1 (LRH-1) in human breast carcinoma: Possible regulator of in situ steroidogenesis. *Cancer Lett.* **2006**, *244*, 24–33. (f) Safi, R.; Kovacic, A.; Gaillard, S.; Murata, Y.; Simpson, E. R.; McDonnell, D. P.; Clyne, C. D. Coactivation of Liver Receptor Homologue-1 by Peroxisome Proliferator-Activated Receptor gamma Coactivator-1.alpha. on Aromatase Promoter II and Its Inhibition by Activated Retinoid X Receptor Suggest a Novel Target for Breast-Specific Antiestrogen Therapy. *Cancer Res.* **2005**, *65*, 11762–11770.(g) Thiruchelvam, P. T.; Lai, C. F.; Hua, H.; Thomas, R. S.; Hurtado, A.; Hudson, W.; Bayly, A. R.; Kyle, F. J.; Periyasamy, M.; Photiou, A.; Spivey, A. C.; Ortlund, E. A.; Whitby, R. J.; Carroll, J. S.; Coombes, R. C.; Buluwela, L.; Ali, S. The liver receptor homolog-1 regulates estrogen receptor expression in breast cancer cells. *Breast Cancer Res. Treat.* **2010**, DOI: 10.1007/s10549-010-0994-9.

(25) Botrugno, O. A.; Fayard, E.; Annicotte, J. S.; Haby, C.; Brennan, T.; Wendling, O.; Tanaka, T.; Kodama, T.; Thomas, W.; Auwerx, J.; Schoonjans, K. Synergy between LRH-1 and beta-catenin induces G(1) cyclin-mediated cell proliferation. *Mol. Cell* **2004**, *15*, 499–509.

(26) Wang, S.-L.; Zheng, D.-Z.; Lan, F.-H.; Deng, X.-J.; Zeng, J.; Li, C.-J.; Wang, R.; Zhu, Z.-Y. Increased expression of hLRH-1 in human gastric cancer and its implication in tumorigenesis. *Mol. Cell. Biochem.* **2008**, *308*, 93–100.

(27) D'Errico, I.; Moschetta, A. Nuclear receptors, intestinal architecture and colon cancer: An intriguing link. *Cell. Mol. Life Sci.* **2008**, *65*, 1523–1543.

(28) Schoonjans, K.; Dubuquoy, L.; Mebis, J.; Fayard, E.; Wendling, O.; Haby, C.; Geboes, K.; Auwerx, J. Liver receptor homolog 1 contributes to intestinal tumor formation through effects on cell cycle and inflammation. *Proc. Natl. Acad. Sci. U.S.A.* **2005**, *102*, 2058–2062.

(29) (a) Mullen, E. M.; Gu, P.; Cooney, A. J. Nuclear receptors in regulation of mouse ES cell pluripotency and differentiation. *PPAR Res.* **2007**, *2007*, article ID 61563. (b) Yang, H.-M.; Do, H.-J.; Kim, D.-K.; Park, J.-K.; Chang, W.-K.; Chung, H.-M.; Choi, S.-Y.; Kim, J.-H. Transcriptional regulation of human Oct4 by steroidogenic factor-1. *J. Cell. Biochem.* **2007**, *101*, 1198–1209.

(30) (a) Heng, J. C. D.; Feng, B.; Han, J. Y.; Jiang, J. M.; Kraus, P.; Ng, J. H.; Orlov, Y. L.; Huss, M.; Yang, L.; Lufkin, T.; Lim, B.; Ng, H. H. The Nuclear Receptor NR5A2 Can Replace Oct4 in the Reprogramming of Murine Somatic Cells to Pluripotent Cells. *Cell Stem Cell* **2010**, *6*, 167–174. (b) Guo, G.; Smith, A. A genome-wide screen in EpiSCs identifies NR5A nuclear receptors as potent inducers of ground state pluripotency. *Development* **2010**, *137*, 3185–3192.

(31) Lee, Y. K.; Choi, Y. H.; Chua, S.; Park, Y. J.; Moore, D. M. Phosphorylation of the hinge domain of the nuclear hormone receptor LRH-1 stimulates transactivation. *J. Biol. Chem.* **2006**, *281*, 7850–7855.

(32) (a) Chalkiadaki, A.; Talianidis, I. SUMO-dependent compartmentalization in promyelocytic leukemia protein nuclear bodies prevents the access of LRH-1 to chromatin. *Mol. Cell. Biol.* **2005**, *25*, 5095–5105. (b) Lee, M. B.; Lebedeva, L. A.; Suzawa, M.; Wadekar, S. A.; Desclozeaux, M.; Ingraham, H. A. The DEAD-Box protein DP103 (Ddx20 or gemin-3) represses orphan nuclear receptor activity via SUMO modification. *Mol. Cell. Biol.* **2005**, *25*, 1879–1890.

(33) (a) Bavner, A.; Matthews, J.; Sanyal, S.; Gustafsson, J. A.; Treuter, E. EID3 is a novel EID family member and an inhibitor of CBP-dependent co-activation. *Nucleic Acids Res.* **2005**, *33*, 3561–3569. (b) Bavner, A.; Sanyal, S.; Gustafsson, J. A.; Treuter, E. Transcriptional corepression by SHP: Molecular mechanisms and physiological consequences. *Trends Endocrinol. Metab.* **2005**, *16*, 478–488.

(34) (a) Iyer, A. K.; McCabe, E. R. B. Molecular mechanisms of DAX1 action. *Mol. Genet. Metab.* **2004**, *83*, 60–73. (b) Sablin, E. P.; Woods, A.; Krylova, I. N.; Hwang, P.; Ingraham, H. A.; Fletterick, R. J. The structure of corepressor Dax-1 bound to its target nuclear receptor LRH-1. *Proc. Natl. Acad. Sci. U.S.A.* **2008**, *105*, 18390–18395.

(35) (a) Ingraham, H. A.; Redinbo, M. R. Orphan nuclear receptors adopted by crystallography. *Curr. Opin. Struct. Biol.* **2005**, *15*, 708–715. (b) Krylova, I. N.; Sablin, E. P.; Moore, J.; Xu, R. X.; Waitt, G. M.; MacKay, J. A.; Juzumiene, D.; Bynum, J. M.; Madauss, K.; Montana, V.; Lebedeva, L.; Suzawa, M.; Williams, J. D.; Williams, S. P.; Guy, R. K.; Thornton, J. W.; Fletterick, R. J.; Willson, T. M.; Ingraham, H. A. Structural analyses reveal phosphatidyl inositols as ligands for the NR5 orphan receptors SF-1 and LRH-1. *Cell* **2005**, *120*, 343–355. (c) Li, Y.; Choi, M.; Cavey, G.; Daugherty, J.; Suino, K.; Kovach, A.; Bingham, N. C.; Kliewer, S. A.; Xu, H. E. Crystallographic identification and functional characterization of phospholipids as ligands for the orphan nuclear receptor steroidogenic factor-1. *Mol. Cell* **2005**, *17*, 491–502. (d) Ortlund, E. A.; Lee, Y.; Solomon, I. H.; Hager, J. M.; Safi, R.; Choi, Y.; Guan, Z. Q.; Tripathy, A.; Raetz, C. R. H.; McDonnell, D. P.; Moore, D. D.; Redinbo, M. R. Modulation of human nuclear receptor LRH-1 activity by phospholipids and SHP. *Nat. Struct. Mol. Biol.* **2005**, *12*, 357–363.

(36) Sablin, E. P.; Blind, R. D.; Krylova, I. N.; Ingraham, J. G.; Cai, F.; Williams, J. D.; Fletterick, R. J.; Ingraham, H. A. Structure of SF-1 Bound by Different Phospholipids: Evidence for Regulatory Ligands. *Mol. Endocrinol.* **2009**, *23*, 25–34.

(37) Moore, D. D.; Lee, J. M. Phospholipid LRH-1 receptor agonist compositions and use for the treatment of metabolic disorders and inflammatory bowel disease and lowering of blood glucose levels. WO 2009067182, 2009.

(38) (a) Urs, A. N.; Dammer, E.; Kelly, S.; Wang, E.; Merrill, A. H.; Sewer, M. B. Steroidogenic factor-1 is a sphingolipid binding protein. *Mol. Cell. Endocrinol.* **2007**, *265*, 174–178. (b) Urs, A. N.; Dammer, E.; Sewer, M. B. Sphingosine regulates the transcription of CYP17 by binding to steroidogenic factor-1. *Endocrinology* **2006**, *147*, 5249–5258. (c) Dammer, E. B.; Leon, A.; Sewer, M. B. Coregulator exchange and sphingosine-sensitive cooperativity of steroidogenic factor-1, general control nonderepressed 5, p54, and p160 coactivators regulate cyclic adenosine 3′,5′-monophosphate-dependent cytochrome P450c17 transcription rate. *Mol. Endocrinol.* **2007**, *21*, 415–438.

(39) Whitby, R. J.; Dixon, S.; Maloney, P. R.; Delerive, P.; Goodwin, B. J.; Parks, D. J.; Willson, T. M. Identification of Small Molecule Agonists of the Orphan Nuclear Receptors Liver Receptor Homolog-1 and Steroidogenic Factor-1. *J. Med. Chem.* **2006**, *49*, 6652–6655.

(40) (a) Fan, W.; Yanase, T.; Morinaga, H.; Gondo, S.; Okabe, T.; Nomura, M.; Hayes, T. B.; Takayanagi, R.; Nawata, H. Herbicide atrazine activates SF-1 by direct affinity and concomitant co-activators recruitments to induce aromatase expression via promoter II. *Biochem. Biophys. Res. Commun.* **2007**, *355*, 1012–1018. (b) Fan, W. Q.; Yanase, T.; Morinaga, H.; Ondo, S.; Okabe, T.; Nomura, M.; Komatsu, T.; Morohashi, K. I.; Hayes, T. B.; Takayanagi, R.; Nawata, H. Atrazine-induced aromatase expression is SF-1 dependent: Implications for endocrine disruption in wildlife and reproductive cancers in humans. *Environ. Health Perspect.* **2007**, *115*, 720–727. (c) Suzawa, M.; Ingraham, H. A. The herbicide atrazine activates endocrine gene networks via non-steroidal

NR5A nuclear receptors in fish and mammalian cells. *PLoS One* **2008**, *3*, e2117.

(41) Madoux, F.; Li, X.; Chase, P.; Zastrow, G.; Cameron, M. D.; Conkright, J. J.; Griffin, P. R.; Thacher, S.; Hodder, P. Potent, selective and cell penetrant inhibitors of SF-1 by functional ultra-high-throughput screening. *Mol. Pharmacol.* **2008**, *73*, 1776–1784.

(42) Roth, J.; Madoux, F.; Hodder, P.; Roush, W. R. Synthesis of small molecule inhibitors of the orphan nuclear receptor steroidogenic factor-1 (NR5A1) based on isoquinolinone scaffolds. *Bioorg. Med. Chem. Lett.* **2008**, *18*, 2628–2632.

(43) Thomas, E.; Dixon, S.; Whitby, R. J. A rearrangement to a zirconium-alkenylidene in the insertion of dihalocarbenoids and acetylides into zirconacycles. *Ange. Chem. Int. Ed.* **2006**, *45*, 7070–7072.

(44) Stec, J.; Dixon, S.; Thomas, E. V.; Whitby, R. J. Tandem insertion of halocarbenoids and lithium acetylides into zirconacycles. A novel rearrangement to zirconium-alkenylidenates via β-addition to an alkynyl-zirconocene. *Chem.—Eur. J.* **2011**, in press.

(45) (a) Abad, A.; Agullo, C.; Arno, M.; Cantin, A.; Cunat, A. C.; Meseguer, B.; Zaragoza, R. J. Stereoselective synthesis of (−)-metasequoic acid B. *J. Chem. Soc. Perkin Trans. 1* **1997**, 1837–1843. (b) Larson, G. L.; Klesse, R. An Improved Synthesis of the Ethylene Acetal of 3-Iodopropanal and the Ethylene Ketal of 4-Iodo-2-Butanone. *J. Org. Chem.* **1985**, *50*, 3627–3627.

(46) (a) Karplus, M. Vicinal Proton Coupling in Nuclear Magnetic Resonance. *J. Am. Chem. Soc.* **1963**, *85*, 2870–2871. (b) Haasnoot, C. A. G.; Deleeuw, F. A. A. M.; Altona, C. The Relationship between Proton-Proton Nmr Coupling-Constants and Substituent Electronegativities. 1. An Empirical Generalization of the Karplus Equation. *Tetrahedron* **1980**, *36*, 2783–2792.

(47) Light, M. E.; Stec, J.; Whitby, R. J. Private communication to the Cambridge Structural Database, deposition number CCDC 746929, 2009.

(48) Diaz, Y.; Bravo, F.; Castillon, S. Synthesis of purine and pyrimidine isodideoxynucleosides from (*S*)-glycydol using iodoetherification as key step. Synthesis of (*S*,*S*)-iso-ddA. *J. Org. Chem.* **1999**, *64*, 6508–6511.

(49) Cink, R. D.; Forsyth, C. J. Facile one-pot epoxidation-nucleophilic opening sequence for vicinal diols. *J. Org. Chem.* **1995**, *60*, 8122–8123.

(50) Wang, L.; Maddess, M. L.; Lautens, M. Convenient access to functionalized vinylcyclopentenols from alkynyloxiranes. *J. Org. Chem.* **2007**, *72*, 1822–1825.

(51) Halgren, T. A. Merck molecular force field. 1. Basis, form, scope, parameterization, and performance of MMFF94. *J. Comput. Chem.* **1996**, *17*, 490–519.

(52) Navarro-Vazquez, A.; Cobas, J. C.; Sardina, F. J.; Casanueva, J.; Diez, E. A graphical tool for the prediction of vicinal proton-proton (3)J(HH) coupling constants. *J. Chem. Inf. Comput. Sci.* **2004**, *44*, 1680–1685.

(53) (a) Wittig, I.; Braun, H. P.; Schagger, H. Blue native PAGE. *Nat. Protoc.* **2006**, *1*, 418–428. (b) Wittig, I.; Schagger, H. Advantages and limitation of clear-native PAGE. *Proteomics* **2005**, *5*, 4338–4346.

(54) Ingraham, H. A. Unpublished results.

(55) Winn, M. D.; Murshudov, G. N.; Papiz, M. Z. Macromolecular TLS refinement in REFMAC at moderate resolutions. *Methods Enzymol.* **2003**, *374*, 300–321.

(56) Emsley, P.; Lohkamp, B.; Scott, W. G.; Cowtan, K. Features and development of Coot. *Acta Crystallogr., Sect. D: Biol. Crystallogr.* **2010**, *66*, 486–501.